

2

Photochromism in the Solid State

Oleksandr S. Bushuyev and Christopher J. Barrett

Department of Chemistry, McGill University, Montreal, Canada

2.1 Molecular Photoswitches in the Solid State

Photochromism is a reversible transformation of two chemical species between two energetic states caused by absorption of visible light or, in a broad sense, any electromagnetic radiation. In principle, any double-well potential system that reversibly cycles between two energetic states by absorption of light can be photochromic (a “photoswitch”). Practical photochromic systems, however, need to cleanly switch without the buildup of unwanted side products and possess a sufficiently high potential barrier as to ensure the reasonable stability of both of the energetic states. Numerous classes of molecules that reversibly isomerize between multiple structural configurations in response to external stimuli fall within the realm of molecular switches. Common examples of photochromic molecular switches are illustrated in Figure 2.1. Some of the most extensively studied small-molecule motifs include (but are not limited to) azobenzenes, whose isomerization between *E* and *Z* conformations about a double bond mimics flapping motions [1–3]; diarylethenes and spiropyrans, in which conformational changes are accompanied by ring-opening or -closing reactions [4–6]; anthracene and coumarin derivatives that reversibly dimerize with one another [7, 8]; and overcrowded alkenes, hydrazones, and imines, which behave as rotors that can revolve about a rigid internal axis [9–12]. Covalent modifications of the parent switch and rotor molecules provide near-infinite opportunities to design alternate isomerization pathways and to tune actuation stimuli. Additionally, noncovalent interactions between molecules such as hydrogen bonding, hydrophobic effects, and π - π stacking enable the construction of dynamic host-guest systems, expanding the versatility of switches via supramolecular self-assembly of two or more components [13]. These dynamic molecules represent the smallest building blocks available

Photomechanical Materials, Composites, and Systems: Wireless Transduction of Light into Work, First Edition. Edited by Timothy J. White.

© 2017 John Wiley & Sons, Inc. Published 2017 by John Wiley & Sons, Inc.

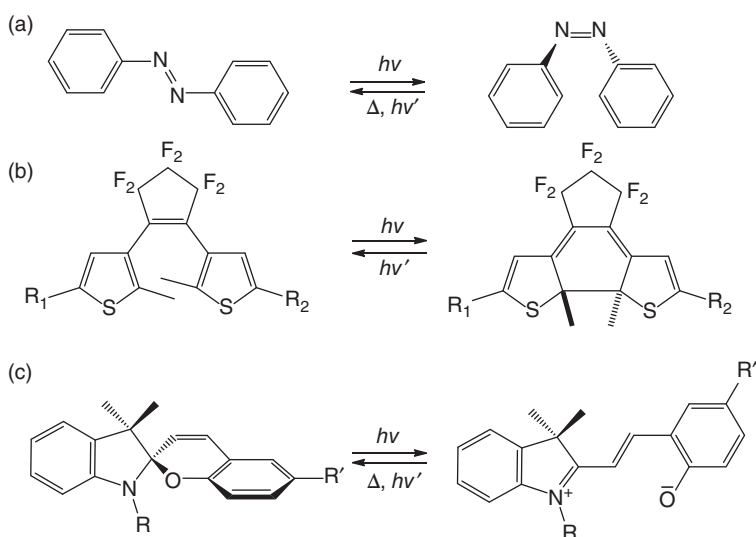


Figure 2.1 Examples of common small-molecule photoswitch isomerization reactions: (a) azobenzenes; (b) diarylethenes; (c) spiropyrans.

for a bottom-up approach to synthesize functional mechanical devices that exhibit motion. While being chemically diverse, all of the aforementioned switch components operate based on similar principles [14], where absorption of a photon manipulates the relative energy barrier between two states.

Photoswitches are usually most extensively studied in solution, where each of the isomerization reactions is most easily characterized and can be considered to occur independently. The focus of this chapter, however, is the reversible transformation of photochromic molecules in the solid state where they are supported by a surface or incorporated into an amorphous polymer host matrix, liquid-crystalline polymer network (LCN), or liquid crystal elastomer (LCE) or grown as single crystals. Typically, chromophores are embedded into a solid matrix both for study and for application as real devices. As a result, matrix effects are inescapable; the behavior of the chromophore is altered due to the matrix, and in turn, the chromophore alters the matrix [15]. Although either could be viewed as a hindrance, both can in fact be quite useful: the chromophore can be used as a delicate probe of the matrix (free volume, polarizability, mobility, morphology, viscoelasticity, etc.), and when the matrix couples to chromophore motion, molecular motions can be translated to larger length scales. An illustrative example of this translation is nanometer-thick “command surfaces” of azobenzene chromophores that can dictate the alignment of micron-thick adjacent layers of otherwise inert liquid crystals [15].

Since the two energetic states of photoswitching molecules exhibit differences in absorption, photochromism, in a literal sense, means a change of color of a material upon absorption of electromagnetic radiation. At the same time, chemical isomerization between the two energetic states can bring about motion and conformational change. In order for a molecule to change conformation, movement of a part or of the whole molecule has to occur. Such molecular motion may be carefully engineered and harnessed to produce a secondary function and enable solid-state photochromism to drive many useful phenomena. The history of photochromism owes much to the azobenzene chromophore; therefore, we cover it in greater detail in the following section.

2.2 Molecular and Macroscopic Motion of Azobenzene Chromophores

Photoinduced motion in azobenzenes, or any other photoswitch, occurs due to the geometric change that occurs upon absorption of light. In *cis*-azobenzene, the phenyl rings are twisted at 90° relative to the C=N=N-C plane [16, 17]. Isomerization reduces the distance between the 4 and 4' positions from 0.99 nm in the *trans* state to 0.55 nm in the *cis* state [18–20]. This geometric change increases the dipole moment: while the *trans* form has no dipole moment, the *cis* form has a dipole moment of 3.1 D [21]. The free-volume requirement of the *cis* form can be much larger than that for the *trans* form [22], and the free volume required to *cycle between* these two states is still larger. It has been estimated that the minimum free-volume pocket required to allow isomerization to proceed through a transition state via the inversion pathway is 0.12 nm^3 [16, 23] and via the rotation pathway is approximately 0.38 nm^3 [24]. The effects of matrix free-volume constraints on photochemical reactions, in general, have been considered [25]. The geometrical changes in azobenzene are very large by molecular standards, and it is thus no surprise that isomerization can modify a wide range of material properties. More recent measurements via high-pressure spectroscopy (10^4 – 10^5 atm) on the force applied and energy exerted through this isomerization suggest that azobenzene is indeed an extremely powerful molecular unit, and employment in actuators depends largely on clever engineering of the mechanical advantage gained and is not inherently material limited.

This molecular displacement generates a significant nanoscale force, which has been measured in single-molecule force spectroscopy experiments [26, 27] and compared well to theory [28]. In these experiments, illumination causes contraction of an azobenzene polymer, showing that each chromophore can exert pN to nN molecular forces on demand. The ability to activate and power molecular-level devices using light is of course attractive in many applications,

since it circumvents the limitations inherent to diffusion or wiring and permits a remote (or even quite distant) power supply. The fast response and absence of side reactions in azo isomerization are also advantageous. Coupling these molecular-scale motions to useful work is of course the next challenging step. To realize this aim, a wide variety of molecular switches have been synthesized and examined. For example, an azo bond linking two porphyrin rings enabled photocontrol of electron transfer [29], and in another example, dramatically different hydrogen-bonding networks (intermolecular and intramolecular) could be favored based on the isomeric state of the azo group linking two cyclic peptides [30, 31]. Other recently reported examples include osmotic pressure pumps [32], created by the photocontrolled solubility of azobenzene, analytical columns that increase the effluent rate of developing solvents [33], reversible light-controlled conductance switching [34], photoresponsive gold nanoparticle solvation [35], and network formation [36].

While it is important to study the nanometer-scale azobenzene molecular conformational changes that give rise to macroscopic phenomena, by far the most useful applications to actuation are the reversible changes that can result in changes to bulk phenomena or to macroscopic motion over the micrometer- to centimeter-size scale. The first consideration is perhaps whether the host material can expand or contract to an appreciable extent. In floating monolayers at a liquid surface, it is well established that the larger molecular size of the *cis* isomer leads to the corresponding lateral expansion of many tens of percentages [37], which can modify other bulk properties. For example, this allows photomodulation of a monolayer's water contact angle [38] or surface potential [39]. Using fluorinated azo polymers, good photocontrol was demonstrated over photopatterning [40, 41], and wettability has been demonstrated [42, 43]. A monolayer of azo-modified calixarene, when irradiated with a light gradient, produced a surface energy gradient sufficient to move a macroscopic oil droplet [15]. In a more recent work, surfactants of azobenzene were used to create a liquid–liquid interface between oleic acid droplets in an aqueous solution [44]. Photoisomerization of the azobenzene surfactant created a wavelength-dependent interfacial tension capable of inducing interfacial flow, and this interfacial flow then generated large-scale droplet motion in a direction opposite to the gradient. The photocontrolled droplet motion was thus used to direct droplets into the trajectories of various shapes and letters. It also suggests possible applications of the aforementioned materials to microfluidics. Modest photoinduced contact angle changes for thin polymer films have also been reported [45]. Recently, an azobenzene copolymer assembled into polyelectrolyte multilayer showed a modest 2° change in contact angle with UV (ultraviolet) light irradiation. However, when the same copolymer was assembled onto a patterned substrate, the change in contact angle upon irradiation was enhanced to 70° [46]. The fact that surface roughness plays a role in contact angle is well established and shows that many

systems can be optimized to give rise to a large change in surface properties through clever amplification.

Perhaps, the most visible demonstration of macroscopic motion induced by the isomerization of azobenzene is the mechanical bending and unbending of freestanding LCN and LCE films [47, 48]. Bending occurs in these relatively thick films because the free surface (which absorbs light) contracts, whereas the interior of the film (which is not irradiated owing to the strong absorption of the upper part of the film) does not contract. Because the direction of bending can be controlled with polarized light, the materials enable full directional photomechanical control [49]. Other examples include expansion–bending of cantilevers coated with an amorphous azobenzene thin film [50] and macroscopic contraction–bending of fibers and cantilevers made of azobenzene liquid-crystalline elastomers [51–57]. One can also invert the coupling of mechanical and optical effects: by stretching an elastomeric azo film containing a grating, one can affect its wavelength-selection properties and orient the chromophores [58].

Depending on the nature of the function and whether it is performed on a micro-, meso-, or macroscopic scale, solid-state macroscopic transformations fall in the realm of photomechanical solids, surface mass transport, molecular machines, or structural changes in network architectures. There is no clear boundary between these classes, as molecular machines perform photomechanical motion, photomechanical materials could be seen as molecular machines scaled up in three dimensions, and surface mass transport effects are not always easily distinguishable from photomechanical motion. Chromophore, as a structural element in different classes of networks, is a fairly new motif that bridges the gaps between all three of these phenomena. We will attempt to categorize the effects, but the reader should also keep in mind the interrelation of these arbitrary classifications. We will mostly discuss molecular machines as surface-organized photochromic molecules performing work in the environment (matrix), while the photomechanical section will cover photochromes in scaled-up freestanding bulk materials such as polymer films and crystals. Mass transport usually occurs close to the surface, while switching inside the networks is typically viewed as a bulk property change. To give the reader a sense of the historical development, we will discuss these effects in chronological order of their discovery and development.

2.3 Photomechanical Effects

The photomechanical effect is a change of shape of a material upon exposure to light (not due simply to heat expansion) and is a property of some materials incorporating light-switchable chromophores. In its essence, it refers to the

direct transformation of light into mechanical motion. For ease of observation and with the goal of maximizing photomechanical efficiency, such materials are generally fabricated into high-aspect-ratio films forming a thin actuator. In the most simple terms, actuators are the systems that convert a given type of stimulus – in this case, energy of photons – into mechanical motion.

If an actuator is defined as an energy transducer converting an input energy into mechanical motion, then azobenzene-based systems are excellent candidates for photomechanical actuation for many niche applications involving small size, localized actuation, remoteness of the power source, and freedom from the encumbrance of batteries, electrons, and internal moving parts. The most convincing demonstration of macroscopic motion due to azo isomerization is the mechanical bending and unbending of freestanding polymer thin films [47, 48]. As the direction of bending can be controlled via the polarization of the light, the materials enable full directional photomechanical control [49] and have been used to drive macroscopic motion of a floating film [59]. For a thin film floating on a water surface, a contraction in the direction of polarized light was seen for LC materials, whereas an expansion was seen for amorphous materials [60]. A related amplification of azo motion to macroscopic motion is the photoinduced bending of a microcantilever coated with an azobenzene monolayer [50]. Other examples include macroscopic bending and three-dimensional control of fibers made of azobenzene liquid-crystalline elastomers [51–53], light-driven micro valves [61], and all-plastic motors [1]. In this section, a survey summary of some of the manifestations of the photomechanical effect leading to macroscale actuation with azobenzene and other photoswitches is provided.

2.3.1 Photomechanical Effects in Amorphous Azo Polymers

Perhaps, not surprisingly, photomechanical effects in organic materials were first noted for the azobenzene chromophore. Merian is often credited with the first observation of the photomechanical effect in azobenzenes, when, in 1966, he observed that an azobenzene-treated nylon filament shrank upon irradiation with a Xe daylight lamp [62]. The relatively unimpressive overall contraction of under 0.1% of the original length and complexity of the sample meant that it was not until 20 years later that anyone took much notice of this curious report. In the 1980s, Eisenbach prepared poly(ethyl acrylate) networks cross-linked with azobenzene chromophore [63]. The samples exhibited photoinduced contraction of around 0.2% upon irradiation with UV light and corresponding expansion after visible light irradiation. Upon further investigations, Matejka *et al.* reported that upon the increase of loading of azobenzene into the material above 5%, a photoinduced contraction of nearly 1% was achieved [64–66].

Thin-film polymer actuators capable of responding to external stimuli and deforming are the most desirable for practical applications, in either

amorphous or organized form (such as liquid crystalline). Photoinduced reversible changes in elasticity of semi-interpenetrating network films bearing azobenzene moieties were achieved by UV and visible light irradiation [67]. These network films were prepared by cationic copolymerization of azobenzene-containing vinyl ethers in a linear polycarbonate matrix. The network film showed reversible deformation by switching the UV light on and off, and the photomechanical effect was attributed to a reversible change between the highly aggregated and dissociated states of the azobenzene groups [67–69]. In other studies, similar films of azobenzene-containing vinyl ethers with polycaprolactone have achieved rapid (0.1 min) anisotropic deformation and recovery. The films, placed under constant tensile stress, were stretched perpendicular and parallel to the tensile stress before irradiation. Photoisomerization of these films resulted in film contraction for stretching parallel to the tensile stress and film elongation for stretching perpendicular to the tensile stress. The photomechanical response was observed to increase with film stretching and was speculated to arise from anisotropic responses caused by the isomerization-induced vibration of azobenzene molecules, which decreases the modulus of the deformed amorphous area [70]. Other polymer films that exhibit high bending intensity and large bending angles (90°) have also been reported [71].

2.3.2 Actuation in Liquid-Crystalline Polymers

In amorphous polymers, photomechanical deformations mostly occur in an isotropic and uniform way, that is, there is no preferential direction for deformation. Anisotropic materials, such as in liquid-crystalline materials, provide direction to the mechanical response. A particularly promising class of materials for efficient photoinduced actuation are LCNs and LCEs. LCEs are lightly cross-linked polymers in which the high alignment order of the mesogens can be coupled with the motions of the highly elastic polymer network. This coupling gives rise to many characteristic properties of LCEs. Upon heating, the alignment order of the LCE films decreases, and when the LC–isotropic phase-transition temperature is exceeded, the films exhibit a contraction along the mesogen alignment direction. Such anisotropic deformation can be very large, and along with the versatile mechanical properties of the polymer network and the reversibility of the process (upon cooling, LCE films revert back to their original size), LCEs show great potential as artificial muscles [72–77].

The application potential of photocontrolled actuators was further promoted when Ikeda *et al.* reported various photoinduced 3D motions (bending) of azobenzene LC gels and elastomers [47, 48, 78]. The bending is driven by a gradient in the isomerization-induced reduction in the LC alignment order: the majority of the incident UV irradiation is absorbed within a relatively thin

surface layer of the film, which generates asymmetric strain and subsequent deformation. The process is reversible: UV irradiation destroys the mesogen alignment through trans–cis isomerization and causes the sample to bend, whereas irradiation with visible green light restores the azobenzenes to the trans form and the film regains its original unbent state. The nature of bending strongly depends on the details of the material system. Homogeneously aligned polymer systems bend in the mesogen alignment direction [78], whereas the bending direction of polydomain LCEs can be controlled by linearly polarized light [47]. The latter serves as an example of repeatable and precisely controlled photoinduced deformation along any chosen direction, enabling full photomechanical directional control. It is an important step toward practical applicability of light-driven actuators. Another example of direction control is provided by artificial muscle-like photochromic fibers, the bending direction of which can be controlled by changing the location of the illuminating source [79, 80]. Conversely, homeotropically aligned cross-linked LC polymer films were observed to exhibit a completely different bending behavior; upon exposure to UV light, they bent *away* from the light source, due to isotropic expansion of the sample surface upon trans–cis isomerization [81]. The initial chromophore alignment is not the only way to control the directionality of the photoinduced bending: Tabiryan *et al.* demonstrated that the bending direction can be controlled with the polarization direction of the excitation beam, which was attributed to light-induced reorientation of the azobenzene moieties [82]. More recently, Van Oosten *et al.* showed that the bending direction can be controlled by designing the material to bear internal composition gradients within the LC polymer network [83], and as the latest example, Shishido and coworkers showed that the bending direction can also be dictated by the nature of bonding between the azobenzene moieties and the cross-linked polymer network [84].

With appropriate engineering, the photoinduced deformations (expansion/contraction and bending) can be translated into “real-life” actuation, to design proof-of-principle micromachines capable of producing applicable work. As the first example of such engineering, Ikeda, with Yamada, Barrett, and coworkers, translated the photoinduced deformations of a cross-linked liquid-crystalline polymer (CLCP) film into rotational motion [1]. They laminated a film of azobenzene with a thin polyethylene sheet, joined two ends of the composite film to create a continuous ring, and mounted it onto a pulley system. Upon simultaneous irradiation with both UV and visible light on each of the pulleys to “pull” and “push,” the belt was driven in counterclockwise rotational motion (Figure 2.2a). Other recent examples by the same research collaboration include an “inchworm” locomotion achieved by attaching a sheet of azo-LCN on a flexible polyethylene (PE) substrate with asymmetric sliding friction [85]. In this application, the film undergoes photomechanical contraction, while the asymmetric end shapes on the PE films act as a ratchet,

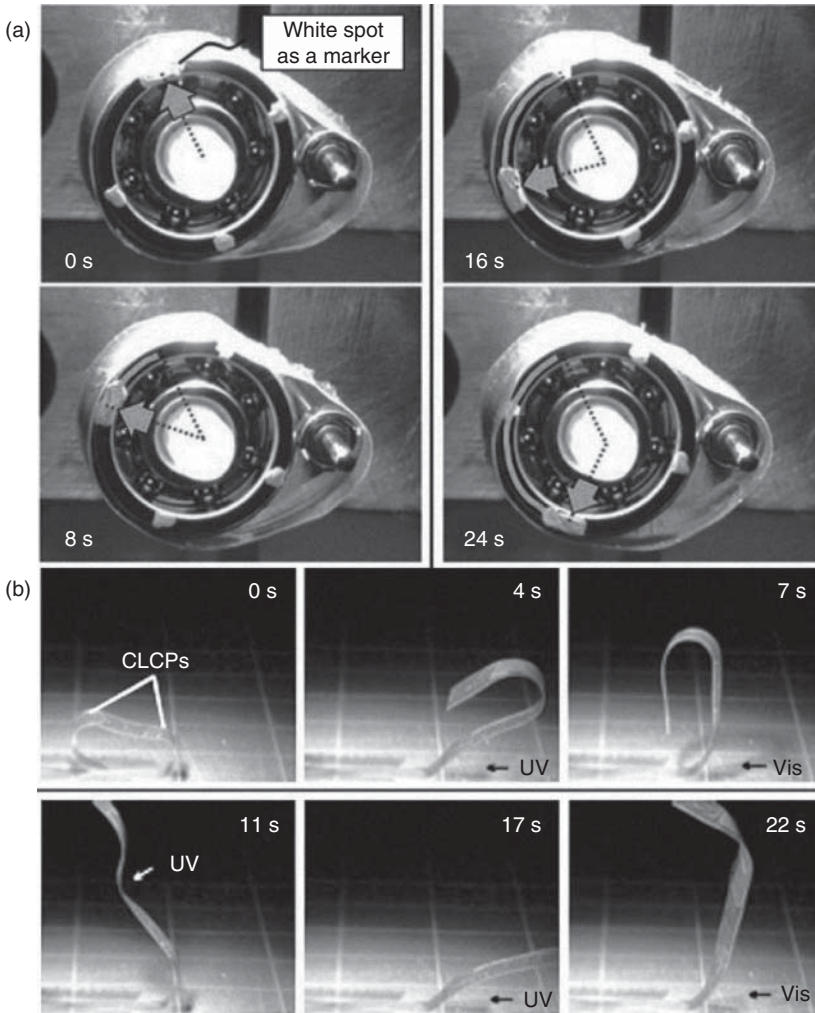


Figure 2.2 (a) Series of photographs showing the rotation of the light-driven plastic motor with the LCE laminated film induced by simultaneous irradiation with UV and visible light. (Yamada *et al.* [1]. Reproduced with the permission of Royal Society of Chemistry.) (b) Series of photographs of the flexible "robotic arm" motion of the azo-LCE laminated film induced by irradiation with UV and visible light. Arrows indicate the direction of light irradiation. (Yamada *et al.* [85]. Reproduced with the permission of Royal Society of Chemistry.)

directing the motion of the film. Robotic arm-like actuation of flexible PE sheets was also demonstrated using azo-polymer “hinges” (Figure 2.2b). Different sections of a flexible PE film were laminated with azo-CLCPs, which enabled specific optical control (expansion or contraction) at various individually addressable positions of the film. The sections containing the azo-CLCPs thus functioned as hinge joints, acting as “arms” with remote control over “elbows” and “wrists.”

The latest advancement addressed an important problem inherent to the laminated azo-CLCP films: even if their mechanical strength is improved by the flexible polymer substrate, the poor adhesion between the two layers prevents efficient deformation transfer from the photoactive layer to the polymer substrate. This can be overcome by connecting the active and passive layers by chemical bonding (using e-beam cross-linking) [86]. The durability of such adhesive-free bilayer structures was significantly improved as compared to adhesive-containing laminated films, and they might provide a route toward increasing the optical–mechanical energy conversion efficiency of the light-driven motors.

In the previous examples of photo-driven motions, the primary energy source was the combination of UV and visible light sources, which gave rise to locally addressable photoinduced contraction/expansion of the photoactive polymer films. UV light is harmful to many living organisms, however, so it is important to develop photo-driven actuators powered by visible light, and ultimately sunlight, for any bio-related applications, and in general, there is an advantage to avoiding UV light to lessen material degradation. The first sunlight-driven photomobile materials, employing photoresponsive azotolane moieties, were developed by Yu and coworkers [87], who also fabricated visible-light-driven microrobots capable of lifting up and moving an object weighing 10 mg, 10 times the weight of the robotic arm itself [57, 88]. This integrated system consisted of several azo-LCN films on PE substrates connected by joints to mimic the arm, wrist, hand, and even fingers of the human arm. The robotic arm could be bent and manipulated to perform complex actions by individually addressing the various photoactive sections, for instance, an object could be picked up or dropped by addressing the “fingers,” while the entire arm could be moved by addressing it at different “elbow” locations. Later on, White and coworkers demonstrated a clever photo-fueled catapult motion, capable of launching an object at a rate of 0.3 m/s using moderate-intensity blue-light irradiation [89]. Yu and coworkers also designed a similar composite material, in which upconverting nanophosphors assisted in inducing the photoinduced deformation using near-infrared (NIR) (980 nm) light [90].

White and coworkers have reported the prospect of high-frequency photo-driven oscillators [51–53]. They designed azo-LCN materials and integrated into cantilevers capable of achieving oscillation frequencies as

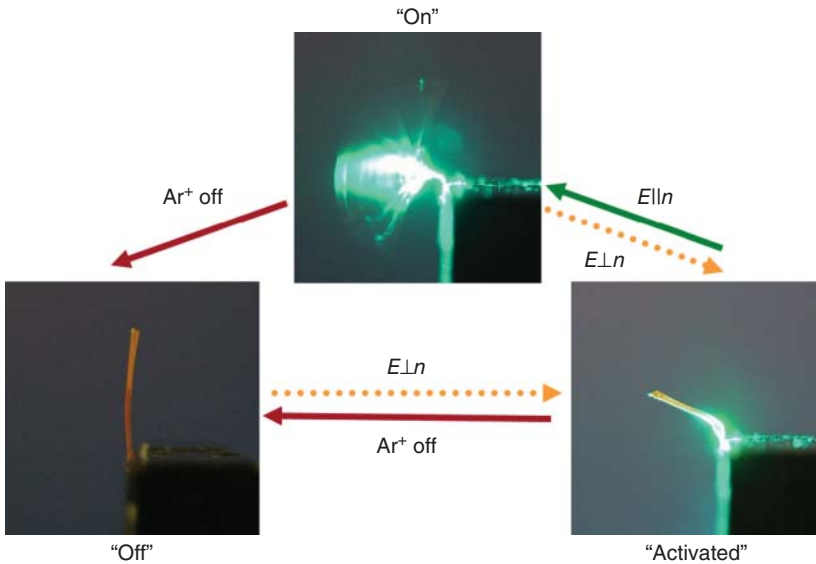


Figure 2.3 The optical protocol for activating the light-powered oscillation of a cantilever. The nematic director (n) is positioned parallel to the long axis of the polymer cantilever of dimension $5 \text{ mm} \times 1 \text{ mm} \times 50 \text{ mm}$. When exposed to light polarized orthogonal to n ($E \perp n$), bending occurs toward the laser source. Cycling the Ar^+ laser from $E \perp n$ to $E \parallel n$ can turn oscillation "on," while blocking the Ar^+ or returning the polarization of the laser beam to $E \perp n$ turns the oscillation "off." (White *et al.* [51]. Reproduced with the permission of Royal Society of Chemistry.) (See color plate section for the color representation of this figure.)

high as 270 Hz and an energy conversion efficiency of 0.1% upon irradiation with a focused blue laser beam, with a range of motion close to 180° (Figure 2.3). The cantilevers possessed a storage modulus ranging from 1.3 to 1.7 GPa and were shown to bend faster and attain larger bending angles with monodomain orientation, increasing azobenzene concentration, and reduced thickness. The bending angle was also dependent on the polarization of the incoming light as well as atmospheric pressure. These cantilevers also oscillated under a focused beam of sunlight [53] and thus offer the potential for remotely triggered photoactuation, adaptive optics, and, most importantly, solar energy harvesting. Such high-frequency oscillators could power a miniaturized micro-opto-mechanical system as they contain both the force generation component (azobenzene) and the kinematic structure (cantilever) in a single unit.

The aforementioned studies employed azo-LCN entirely composed of azobenzene mesogens. In such systems, practically all of the incident irradiation is absorbed within the near-surface region with a thickness of $1\text{--}2 \mu\text{m}$. As typical film thicknesses used are in the order of $10\text{--}20 \mu\text{m}$, the majority of

the azobenzene moieties in the bulk of the film remain dark and unaffected by incident light. As a result, the efficiency of the photomechanical effect generated in such plain-azobenzene actuators is far from optimal. This was first addressed by Broer and coworkers, who designed densely cross-linked high-elastic-modulus polymer actuators with relatively low azobenzene concentration [91]. Indeed, as shown by Palfy-Muhoray and coworkers as early as in 2004, even nonphotoresponsive LCEs *doped* with low concentrations of azobenzene dyes can exhibit remarkable and unprecedented photoinduced deformation behavior [59]. In fact, it has been recently shown that the optimum photoinduced response (in terms of the stress generated) is achieved using a moderate concentration of azobenzene moieties, supplemented with higher concentrations of nonphotoactive mesogens [92]. The largest mechanical force generated by photoirradiation of the various films was measured as 2.6 MPa. Detailed studies have also been performed on the cross-linker concentration dependence of azo-LCN. The cross-linking density changes the elastic modulus and the thermomechanical properties of the material system in a delicate manner, playing an important role in the mobility of the polymer segments, and in general, low cross-linker concentration is favorable for optimizing the photoinduced/thermally induced deformation of cross-linked LC polymers, whereas high cross-linker concentration (high modulus) is preferable for high photoinduced stress generation [76, 93, 94]. A recent observation by Shishido and coworkers suggests that the photoinduced bending of azo-CLCPs is accompanied by a significant, 2.5-fold decrease in the Young's modulus of the sample upon UV irradiation [94]. Such "photo-softening" was observed to be the most pronounced in a low-cross-linker-concentration (and low-modulus) sample, which also exhibited the most efficient photoinduced bending. Upon increasing the cross-linker concentration (and the modulus), both photoinduced bending and the photo-softening effect became less efficient, indicating that there might be a profound connection between the photo-softening and the photomechanical properties of azo-LCNs. In order to probe such connections further, the Broer group offered a route to maximize photo-expansion and, consequently, photomechanical bending [95]. They found that higher expansion was possible upon simultaneous irradiation of an azo-LCN with UV and visible light, stimulating dynamic *trans*↔*cis* conversion and enhancing the free volume of a system by a factor of 4. Surface protrusions as high as 12% were achieved on these azo-LNC films compared to just a 3% expansion upon single wavelength irradiation.

More recent notable advances in the field of photomechanical polymers report on the development of more complex movement patterns, designs that respond to a broader range of stimuli, and better addressability or spatial precision [96, 97]. Katsonis and coworkers, for example, recently described impressive control over the helical motion of azobenzene-containing liquid-crystalline polymer springs, mimicking the extensile function of plant

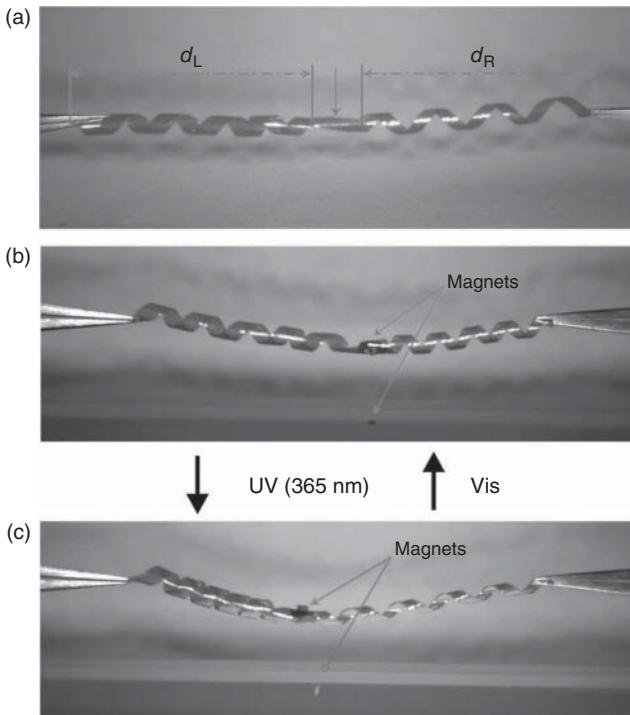


Figure 2.4 The central kink in the mixed helicity ribbon (a) incorporating azobenzene chromophore undergoes a piston-like shuttling motion upon irradiation with visible (b) and UV (c) light. A magnet is connected to the kink and is transported and transmits the push–pull shuttling motion to a second magnet placed 10 mm below. (Iamsaard *et al.* [98]. Reproduced with the permission of Nature Publishing Group.)

tendrils [98] (Figure 2.4). The helical deformations were preprogrammed by including chiral azobenzene dopants and control of the relative orientation of the aligned liquid crystals within each spring, respectively. Chiral dopants induce a left-handed and right-handed twist in the liquid-crystalline film. Depending on the direction, in which such a film is cut, it will curl, twist, or do both upon irradiation with light. Complex extensile and contractile coiling and twisting helical motions are possible, and mechanical energy can be exported from the system by the use of a pair of magnets.

2.3.3 Photosalient, Photochromic, and Photomechanical Crystals

While polymeric materials offer ease of processing and fabrication, crystalline motifs offer a path to near-perfect three-dimensional arrangements of dynamic molecular building blocks as well as a facile means to monitor the motion of the crystals using nuclear magnetic resonance (NMR) and X-ray diffraction.

Furthermore, energy transduction in crystals is faster, and actuating motion is generally of larger magnitude compared to polymeric assemblies because rigidly packed molecules have to work as a cooperative assembly, whereas in a less-ordered medium, motion of the same molecular switches may be less directionally biased and ultimately less efficient. Often derided as a “chemical cemetery” after Leopold Ruzicka’s famous remark, crystal machines instead have witnessed a remarkable resurgence in recent years with discoveries of controlled or spontaneous actuation, reversible or irreversible movements, and reactivity [99–101]. Entire crystals of photochromic molecules can serve as actuators and convert the external stimulus such as light into mechanical energy. Depending on the photomechanical response, such crystal actuators can be categorized as photosalient or photomechanical crystals [75, 102, 103]. Photosalient crystals are an interesting subset of the more general thermosalient material class, which exhibit spontaneous actuation (jumping) upon heating or irradiation. Thermosalient crystals developed by Naumov and coworkers harness the energy of polymorphic transformations that occur upon heating of crystals. The effect is driven by extremely rapid anisotropic expansion and contraction of the unit cell axes upon a phase transition that was found to be 10^4 times faster than regular crystal-to-crystal phase transformations [104]. This class of crystalline compounds is comprised of a diverse range of materials including brominated organic molecules, terephthalic acid, and organometallic complexes [105, 106]. Although there exists little directional control or foresight into which compounds will exhibit the effect, the explosive “popcorn” crystals nonetheless exhibit impressive centimeter-scale jumping movements that greatly exceed the crystal dimensions. Light-activated chemical processes within crystals, such as changes in the coordination sites of small ligands or [2 + 2] cycloaddition reactions, have also been shown to result in “popping” under UV irradiation [102, 107]. Similarly to thermosalient materials, little control is possible over “popping” crystals, and thus, their utilization as functional molecular machines is difficult to envisage. To circumvent this problem, Sahoo *et al.* developed smart hybrid materials that incorporate thermosalient microcrystallites on flexible sodium caseinate films to impart directionality to the crystals’ movements [108]. The material represents a successful marriage of crystals to biocompatible polymeric films in one system, combining the benefits of the plasticity of soft polymers and the efficient, fast actuation of leaping crystalline solids.

Photomechanical materials can move, bend, twist, or curl when exposed to light in a wider variety of motions and usually with greater control. Some of the most promising photomechanical crystalline systems for converting light into mechanical work have been proposed by Irie and coworkers and are based on diarylethene photoswitches [109]. Light absorption triggers pericyclic ring-opening and -closing reactions of this photoswitch throughout the crystal and is responsible for expansion and contraction, respectively, of the unit cell

that consequently leads to photomechanical bending of the crystal. Structural studies on crystals of diarylethene derivatives link the initial speed of curvature change to crystal thickness [110]. The bending behavior is also dependent on the crystallographic face that is irradiated, which is attributed to differences in molecular packing. While the geometric change that occurs during the isomerization of a single diarylethene photoswitch is modest, the collective action of arrays of molecules in the crystal lattice can produce macroscopic motion. If smartly engineered, such actuating crystals can perform work pushing or lifting objects many times their weight [109, 111], rotating gears [112], or acting as an electrical circuit switch (Figure 2.5) [113].

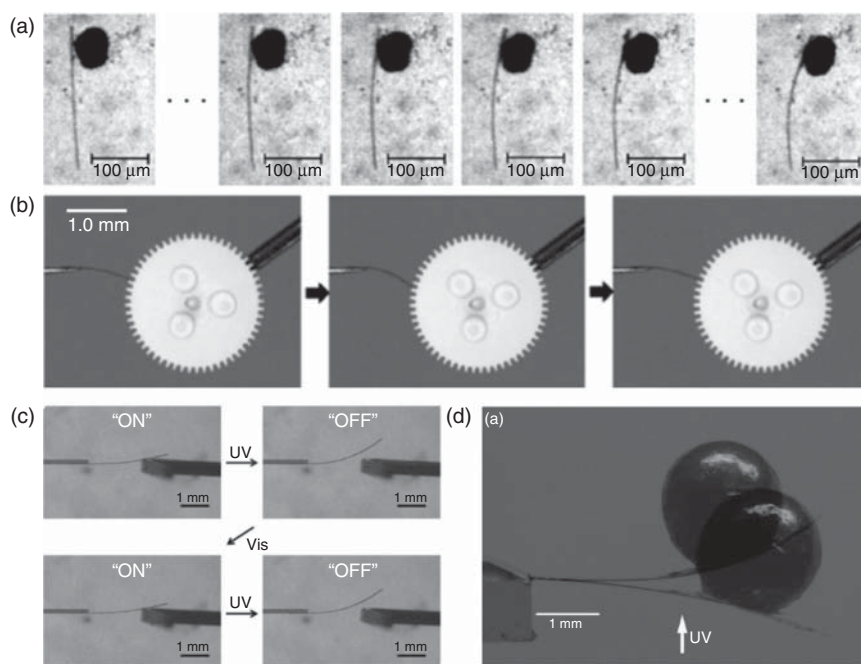


Figure 2.5 Photomechanical systems based on diarylethene crystals that convert light into mechanical work. (a) A rod-like crystal pushes a gold microparticle that is 90 times heavier than the crystal when irradiated with UV light. Bending of the crystal pushes the microparticle up to 30 μm . (Kobatake *et al.* [109]. Reproduced with the permission of Nature Publishing Group.) (b) Rotation of gears facilitated by the reversible bending of a crystalline actuator upon UV and visible irradiation. (Terao *et al.* [112]. Reproduced with the permission of John Wiley and Sons.) (c) Irradiation of gold-coated diarylethene crystals with UV and visible light enables the ON/OFF photoreversible current switching of an electric circuit. (Kitagawa and Kobatake [113]. Reproduced with the permission of Royal Society of Chemistry.) (d) Superimposed photographs of a crystal cantilever lifting a lead ball with a mass 275 times larger than that of the crystal upon irradiation with UV light from the underside of the actuator. (Morimoto and Irie [111]. Reproduced with the permission of American Chemical Society.)

Other commonly studied photomechanical crystalline architectures are composed of anthracenes or salicylidenephenylethylamine molecules. Bardeen and coworkers investigated the [4 + 4] dimerization reaction of anthracenes where the photoreaction results in reversible or irreversible twisting of crystalline microribbons [114, 115]. The curling and twisting motion may be attributed to strain between spatially distinct reactant and product domains as a result of differential absorption by different regions of the crystal or intrinsic solid-state reaction kinetics [116]. Another crystalline molecular machine was proposed by Koshima *et al.* based on photomechanical action in plate-like crystals of salicylidenephenylethylamine (Figure 2.6) [117].

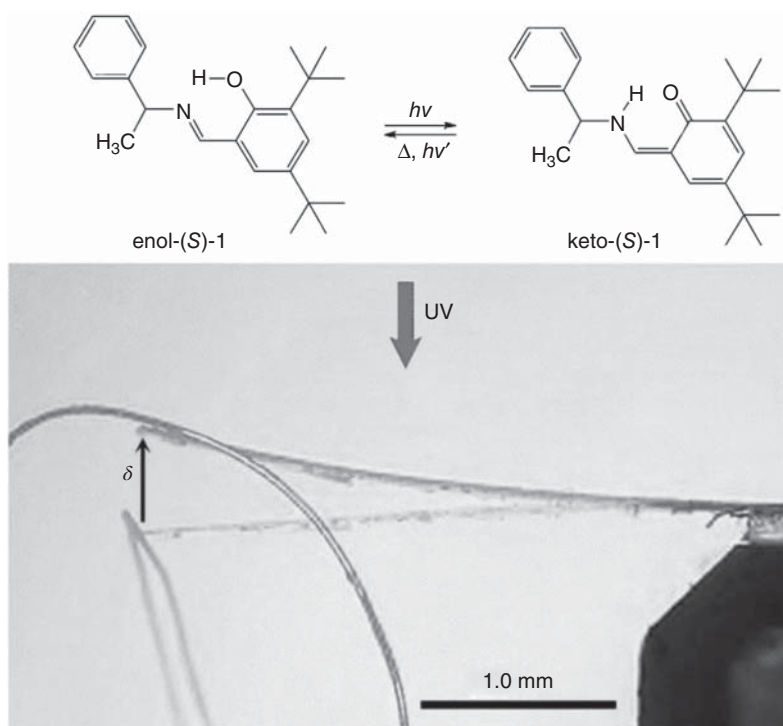


Figure 2.6 (a) Photoinduced proton transfer in the *S* enantiomers of chiral salicylidenephenylethylamines upon keto-enol tautomerism. (b) Superimposed photographs of a chiral enol-(*S*)-1 crystal before and after irradiating the top of the crystal actuator with ultraviolet light. The crystalline cantilever achieved 26 nJ of work by lifting a 4.00 mg metal ring a height, δ , of 0.65 mm. Various photomechanical lifting works were achieved with different enantiomeric compositions within the crystal: the racemic crystal, enol-(*rac*)-1, achieved 59 nJ of work by lifting a weight with a mass 300 times larger than that of the crystal (not shown). (Koshima *et al.* [117]. Reproduced with the permission of American Chemical Society.)

These actuators are capable of lifting weights up to 300 times the mass of the lever. The motion is linked to geometric changes in the molecules produced upon tautomeric transformation triggered by light absorption and consequent proton migration. Collective reorganization of the molecules within the lattice leads to small uniaxial cell expansion, which in turn results in bending of the crystal.

While, perhaps, being the workhorse molecule of most photomechanical studies, the azobenzene chromophore has been extensively investigated mainly on surfaces, in polymers, and within liquid crystals, but it has been far less frequently studied by the crystalline photomechanical community [118–122].

This is due, in part, to the sterically demanding *trans*-to-*cis* isomerization process, which may be impeded in a crystal. Surprisingly, Koshima *et al.* demonstrated reversible photomechanical bending of thin *trans*-4-(dimethylamino)azobenzene plates upon UV irradiation, concluding that isomerization can still occur inside the crystal [123]. That report was followed by a study of thin crystalline plates and needles of pseudostilbenes (azobenzenes with short-lived *cis*-states), which were capable of submillisecond bending and relaxation upon irradiation with visible light [124]. Pseudostilbene bending crystals offer the fastest speed of bending–relaxation cycles as the whole event can take less than a second and is the only system that completely circumvents the need for UV light to induce isomerization. More recent reports have focused on elucidating the mechanistic aspects of azobenzene isomerization in crystals focusing on *in situ* X-ray diffraction studies of irreversible *cis*–*trans* isomerization in crystals [125], and cocrystals [126], of the molecule (Figure 2.7).

These reports demonstrated that *cis*→*trans* isomerization in crystals is mediated by a transient amorphous state. While the sterically demanding azobenzene isomerization reaction requires considerable free volume to occur and is rarely possible in a single-crystal-to-single-crystal manner, an amorphization mechanism enables the photochemical reaction to proceed despite the constraints of the crystal lattice. Amorphous intermediates in the crystal were corroborated by the loss of diffraction spots upon irradiation with visible light at a low temperature. Remarkably, isomerization within the crystals of azobenzene represents a topotactic process in which the orientation of the resultant *trans* crystal phase is dependent on the initial crystal orientation and effectively represents templated crystal growth directed by light.

The growing number of investigations on dynamic molecular crystals that can perform as actuators demands new theoretical models, as will be described in detail in Chapter 3. Various models have been reported in the context of polymer films, rods, or plates, such as the analysis by Warner and Mahadevan on photodeformation of nematic elastomers [127]. However, careful structural and kinetic considerations based on the spatial density and uniform orientations of photoactive molecules must be taken into account for these models to be

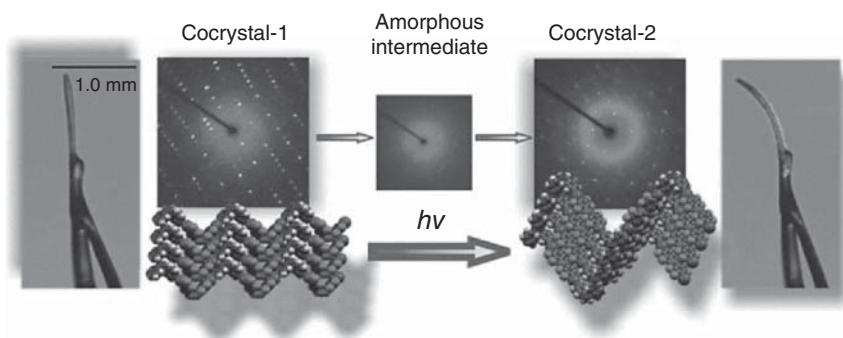


Figure 2.7 Amorphous phase-mediated azobenzene isomerization and photomechanical bending in a cocrystal ($1.2 \text{ mm} \times 90 \mu\text{m} \times 20 \mu\text{m}$). The cocrystal contains a 1:1 ratio of a halogen bond acceptor (*cis*-1,2-bis(4-pyridyl)ethylene) and halogen bond donor species. Bromine or iodine atoms on perfluorinated azobenzenes act as halogen bond donors, having a linear interaction with the pyridine nitrogen atoms on the halogen bond acceptor. Irradiation of the cocrystals with a 532-nm laser facilitates *cis*-to-*trans* isomerization of the halogen bond donors, via amorphous intermediates, determined by X-ray diffraction. (Bushuyev *et al.* [126]. Reproduced with the permission of Royal Society of Chemistry.)

fully applicable to crystalline systems. While the molecular motifs responsible for crystal motions are diverse, an attempt to unify photomechanical processes was made by Nath *et al.*, who proposed a mathematical treatment of photomechanical crystal bending by accounting for the gradual profile of the product in the crystal, irradiation time, direction, and power using the azobenzene dye, Disperse Red 1 (DR1), as a model compound [128]. The model is applicable for any photomechanical crystal system and should allow for an easier comparison between the different platforms for efficiency, modulus, stress, and other parameters critical for optimization of the process for practical use. Ultimately, with the help of theoretical frameworks and empirical data, the goal of future development of photomechanical systems needs to be directed toward robust and fatigue-resistant designs capable of even faster and reliable actuation over thousands of cycles.

2.4 Solid-State Photochromic Molecular Machines

Inspired by the complexity and hierarchical organization of biological machines, the design of artificial molecular machines that exhibit controlled mechanical motion and perform sophisticated tasks is an ultimate pursuit of molecular-scale engineering [129]. The design and synthesis of molecules that can undergo reversible structural changes with various stimuli have received considerable attention, but there remain far fewer reports of dynamic molecular systems such as cleverly designed motors and pumps where the

mechanistic action of their molecular components has been exploited to do controlled work in their environment. The very definition of a machine has been debated ever since biochemistry Professor Isaac Asimov began to lay out the early laws of robotics over 75 years ago in his storytelling [130]. In an effort to advance the field, a stringent language has been sought to differentiate simple molecular switches from motors that are capable of driving a system away from equilibrium [131, 132]. While the working principles of these molecular devices cannot be easily compared to macroscopic analogs, a *molecular machine* has been defined as a multicomponent system with defined energy input that is capable of performing a measurable and useful secondary function either at the nanoscale or, if amplified through collective action, at the macroscale [133]. The system should ideally act in a reversible manner, with the capacity to complete repeated mechanical operations. Spatial and temporal control over this motion and work performed are further hallmarks of successful machines, helping in differentiating deliberate actuated mechanics that leverage Brownian motion from undirected thermal effects and distinguish useful machines from simple molecules that wiggle or diffuse randomly.

The most exciting recent reports on molecules and assemblies exemplify practical and advantageous attributes that can be applied to other systems and show the most promise in successfully advancing the development of artificial molecular machines. Ultimately, the precise and robust integration into higher dimensional architectures that take advantage of mechanical action by many components is essential to bridge the gap between actuating molecular motion and performing microscopic, mesoscopic, and macroscopic work.

2.4.1 Nanostructure Functionalization

The integration of switchable molecular systems into inorganic nanostructures and nanoparticle assemblies enables the manipulation of the hybrid material's optical properties *in situ*. Two common methods to direct the optical properties of nanostructured materials are the active tuning of refractive indices at the surface of plasmonic nanoparticles functionalized with switchable molecules [134–136] and physically modulating interparticle distances or orientations [137]. The intelligent functionalization of larger organic or inorganic nanostructures with small molecular switch and rotor components expands the versatility of these dynamic systems for applications such as drug delivery and for tuning the chemical and physical properties of the hybrid materials [138, 139]. Exemplary demonstrations of artificial molecular machineries that employ functionalized nanostructures include mesoporous nanocrystals modified with molecular nanoimpellers, valves, or gates for the capture and release of cargo with external control [140].

Numerous switch motifs have been utilized as “gatekeepers” to control payload release from these versatile materials including coumarins [141, 142]

and azobenzenes [143, 144]. Besides the necessity for biocompatibility, tissue specificity, and high loading capability, to implement these systems *in vivo* for biomedical applications such as controlled drug release, noninvasive actuation mechanisms are also required because some stimuli may be detrimental to biological environments [145]. In a recent example, a nanoimpeller system developed by Croissant *et al.* utilizes azobenzene photoisomerization as a driving force to release the anticancer drug camptothecin from mesoporous silica nanoparticles (Figure 2.8) [146].

Contrary to classic designs in which azobenzene trans-to-cis isomerization is triggered by UV light (which is harmful to living cells), this system is based on two-photon excitation (TPE) of a fluorophore with NIR light. The use of NIR light facilitates isomerization of the azobenzene moieties through Förster resonance energy transfer (FRET) from a nearby fluorophore. Isomerization of the azobenzene nanoimpellers subsequently kicks out the camptothecin cargo, leading to cancer cell death *in vitro*. Using TPE with NIR light to trigger drug release from mesoporous nanoparticles has not yet been extensively explored but offers the benefits of deeper tissue penetration in the biological spectral window (700–1000 nm) and lower scattering loss [147, 148]. The TPE-based designs illustrate how the actuated mechanics of photoswitches can be tailored by their immediate surroundings by coupling simple switches or rotors to their nanostructured environment, provided that the fluorophores have large two-photon absorption cross sections and sufficient emission quantum yields (>0.5) for FRET.

Azobenzene chromophores hold much promise for application as artificial muscles through linear polymerization, placing the azo photoswitch directly into the polymer backbone instead of just the side groups. By incorporating azobenzene within the main chain of a linear assembly, the culmination of modest dimensional changes of merely a few Ångström for each chromophore can amplify in concert and result in dramatic changes in the contour length of the polymer. Utilizing this strategy, Gaub and coworkers demonstrated the capability of individual polyazobenzene peptides to perform mechanical work by tethering one end of the chain to a substrate and the other to a flexible cantilever to measure the force exerted by the contracting polymer upon photoisomerization [26]. The extent of polymer deformation, and thus the usefulness of the molecules for optomechanical applications, depends on both the conformational rigidity of the backbone and minimization of electronic coupling between azobenzene moieties [149]. The synthesis of rigid-rod polymers that include azobenzene within a poly(*para*-phenylene) backbone is one strategy to maximize photodeformation, enabling accordion-like compression and extension of chains upon cycling with UV and visible light (Figure 2.9a) [150]. Lee and coworkers demonstrated that these single-chain polymeric assemblies may even exhibit crawling movements when deposited onto an octadecylamine-modified graphite surface and imaged with scanning

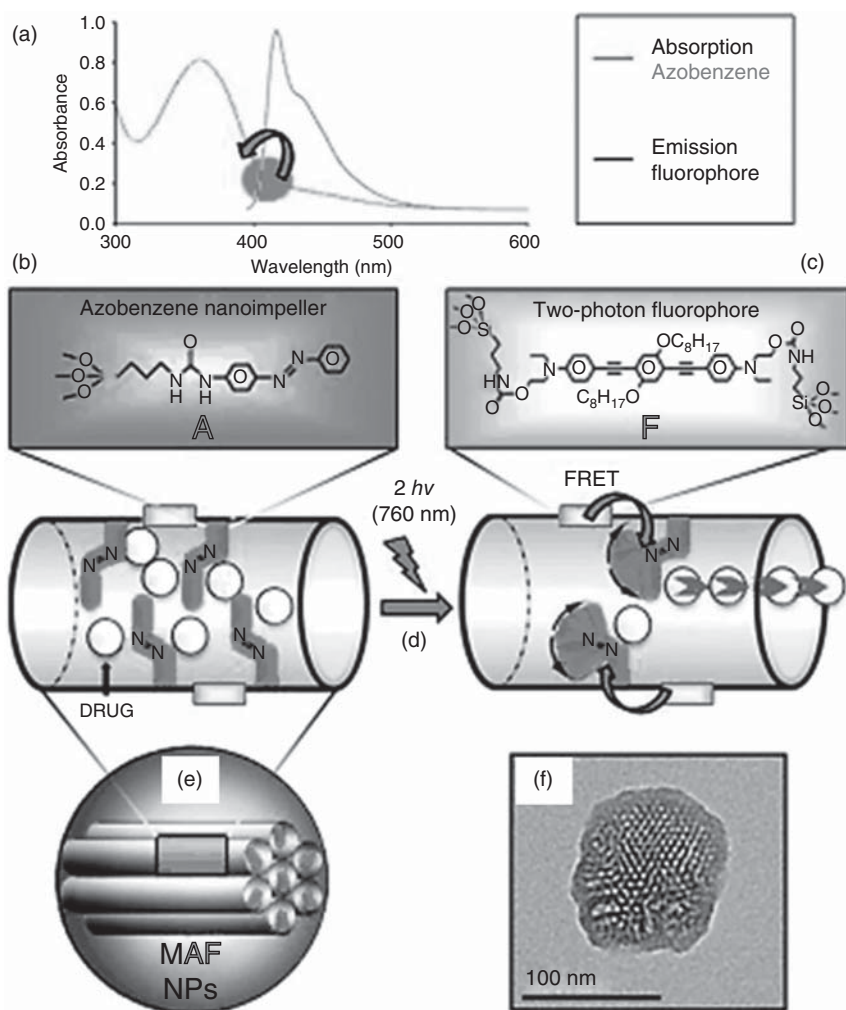


Figure 2.8 Two-photon excitation (TPE) of a fluorophore to facilitate Förster resonance energy transfer (FRET) to photoisomerize azobenzene nanoimpellers on mesoporous silica nanocrystals and subsequent cargo release. (a) Overlap of the emission spectrum of the fluorophore and absorption spectrum of the azobenzene nanoimpeller enables FRET. (b) The chemical structure of the fluorophore. (c) Structure of the two-photon fluorophore. (d) Photoisomerization of azobenzene using two-photon (760 nm) excitation of the fluorophore. (e) Schematic of the mesoporous silica nanocrystal. (f) Transmission electron microscopy image of a single nanocrystal. Light-activated nanovalves that utilize near-infrared irradiation such as this TPE-based mechanism show promise for targeted drug delivery applications and should be further explored to extend their scope. (Croissant *et al.* [146]. Reproduced with the permission of John Wiley & Sons.)

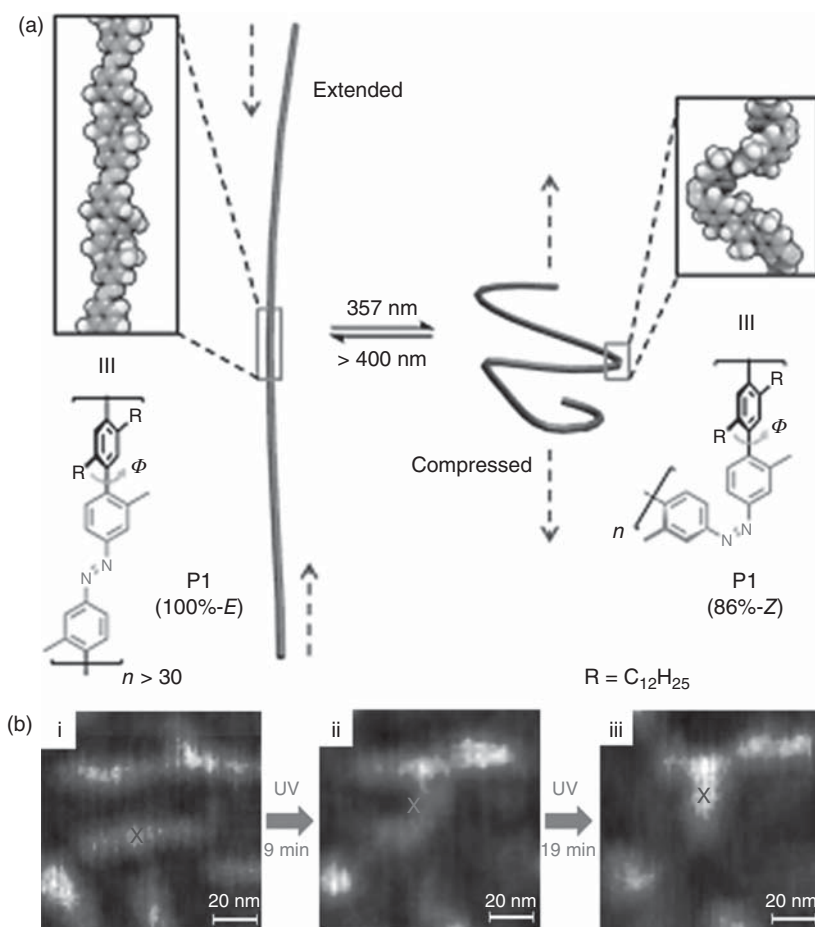


Figure 2.9 (a) Schematic of a main-chain azobenzene-containing polymer (P1; $R = C_{12}H_{25}$) with a poly(*para*-phenylene) backbone. Irradiation with ultraviolet (UV) or visible light facilitates photoisomerization of azobenzene and conversion to the compressed and extended conformations, respectively. (Bleger *et al.* [150]. Reproduced with the permission of John Wiley & Sons.) (b) Scanning force microscopy images of P1 deposited on a modified graphite surface. The polymer crawls along the surface as it contracts upon UV irradiation. Demonstrating control over movement direction and the functionalization or tethering of the polymer strands to scaffolds may enable the macromolecules to perform work by lifting weights or transporting cargo. (Lee *et al.* [151]. Reproduced with the permission of ACS Nano.)

force microscopy (Figure 2.9b) [151]. Chemically or physically cross-linked supramolecular assemblies of these linear photomechanical polymers may be envisioned to behave as actuators, to lift weights, and to perform other types of work with greater resistance to deformation fatigue compared to individual strands [152]. For example, Fang *et al.* reported on using a simple melt spinning method to fabricate hydrogen-bonded cross-linked fibers of azobenzene-containing main-chain polymers that were prepared via a Michael addition reaction (Figure 2.10) [153]. The authors also investigated the photoinduced mechanical properties of the fibers, reporting a maximum stress generated by a single fiber of 240 kPa upon UV irradiation at 35 °C. This force is similar to the maximal tension forces of some chemically cross-linked azobenzene-containing polymer fibers and even human striated muscles (*ca.* 300 kPa) [80].

2.4.2 Two-Dimensional Assemblies and Surface Functionalization

To leverage the mechanical motion of ensembles of molecules, directionality is mandatory to overcome the chaotic (isotropic) generation and application of force. Similarly to Archimedes' need for a place to stand to move the Earth with a lever, a surface may be utilized to instill directionality to harness the power of large numbers of photochromic molecular machines. Two-dimensional coverage by molecular switches and rotors on planar surfaces provides advantages

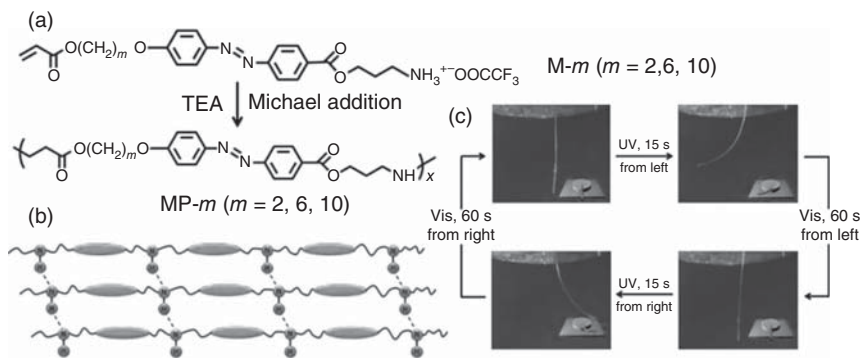


Figure 2.10 (a) Synthetic route and chemical structures of acrylate-type azobenzene monomers. (b) Supramolecular hydrogen-bonding interactions between main-chain polymers to facilitate physical cross-linking. (c) Photographs of a polymeric fiber fabricated by simple melt spinning. The fiber reversibly bends upon irradiation with ultraviolet and visible light. The fibers demonstrate robust photodeformation fatigue resistance and high thermal stability and show promise for applications as photomechanical actuators. (Fang *et al.* [153]. Reproduced with the permission of American Chemical Society.)

over isolated molecules or functionalized nanoparticles by facilitating the manipulation of physical and chemical properties of a material at the micro-, meso-, and macroscales. For example, through the amplification of collective molecular mechanical motion, the integration of small-molecule switches and rotors into ordered arrays has resulted in dynamic control over work function, refractive index, and surface wettability [41, 154–157]. Molecular pumps based on host–guest interactions composed of cyclodextrin and azobenzene designed by Sen and coworkers perform such a function by external stimulation with light [158]. These hybrid systems are organized within gels or adsorbed directly on glass substrates (Figure 2.11a and b). Upon UV light absorption, azobenzene molecules isomerize and leave their cyclodextrin hosts. The created cavity is then promptly filled with water molecules. The amplified and collective actions of the multitude of neighboring pumps create a steady flow of fluid around the surface at a rate of about $2\ \mu\text{m/s}$ (Figure 2.11c and d). The pump can also be activated by chemical stimuli and recharged by visible light irradiation. Despite these impressive examples, there exist few reports on the integration of molecular switches and rotors in planar assemblies because of the challenging design rules that accompany surface functionalization, as described as follows. Self-assembled monolayers (SAMs), Langmuir–Blodgett (LB) films, and layer-by-layer (LBL) assemblies are all relatively well-understood organic thin-film technologies that can be employed to fabricate nanoscale functional surfaces [159]. Within SAMs, intermolecular distances, molecular orientation, and substrate–molecule interactions strongly influence whether assembled switches and rotors retain their functionality due to the varied chemistries of their interfaces [160]. Physically and electronically decoupling these functional moieties from surfaces or from neighboring molecules is often necessary to avoid steric constraints or quenching of excited states [138, 161, 162]. For example, molecular rotors can be tethered such that the axis of rotation is aligned parallel or perpendicular to the surface, in either altitudinal or azimuthal orientations, respectively. Feringa and coworkers reported the tunable and reversible wettability of gold surfaces modified with SAMs of altitudinal rotors based on light-driven overcrowded alkenes bearing perfluorinated alkyl chains [163].

Taking advantage of unhindered rotation enabled by the superior altitudinal orientation of the rotor units dramatically modified the surface energy with resulting water contact angle changes of as much as $8\text{--}22^\circ$ owing to differences in the orientation of the hydrophobic perfluorobutyl group. The photoconversion efficiency and rotation speed of these surface-bound rotors are still generally lower than those for free molecules in solution, highlighting how proper spatial arrangement and sufficient room to rotate are necessary parameters to optimize these dynamic molecular motifs to retain their large-scale functionality [164].

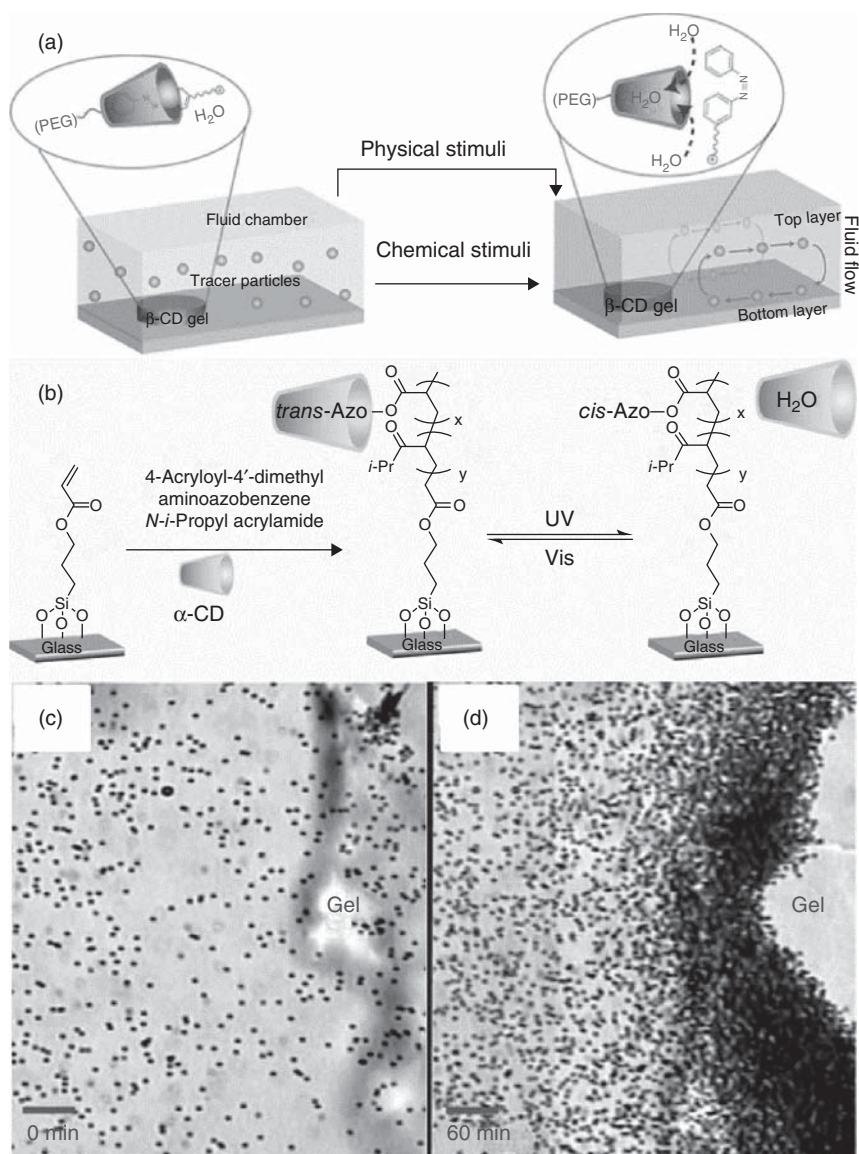


Figure 2.11 (a) Schematic of a dual-responsive micropump on a glass surface. Light or chemical stimuli may be used to induce fluid flow by a β -cyclodextrin–polyethylene glycol (β -CD-PEG) gel upon isomerization of the azobenzene moiety. (b) Schematic of the direct functionalization of glass surfaces by covalently tethering azobenzene-containing molecules. Reversible formation or disassociation of the host/guest complex with α -cyclodextrin results in fluid pumping. (c) Optical microscopy image of tracer particles in solution above a β -CD-PEG gel on a glass surface before irradiation. (d) Optical microscopy image of tracer particles accumulating at the edge of a β -CD-PEG gel after irradiation with ultraviolet light for 1 h. Scale bars, 50 μm . The reversibility of the host/guest interaction makes the design particularly appealing for rechargeable microdevices. (Patra *et al.* [158]. Reproduced with the permission of American Chemical Society.)

2.5 Surface Mass Transport and Phase Change Effects

In 1995, an unexpected and unprecedented optical effect was discovered in polymer thin films containing the azo chromophore DR1. The Natansohn/Rochon research team [165] and the Tripathy/Kumar collaboration [166] simultaneously and independently discovered a large-scale surface mass transport when the films were irradiated with a light interference pattern. In this experiment, two coherent laser beams with a wavelength in the azo absorption band are intersected at the sample surface to interfere. The sample usually consists of a thin spin-cast film (10–1000 nm) of an amorphous azo polymer on a transparent substrate. The sinusoidal light interference pattern at the sample surface leads to a sinusoidal surface topology patterning, that is, a relief grating often referred to in the literature as a surface relief grating (SRG), though the effect is not limited to just gratings, and might more accurately and generally be called photopatterning, phototransport, or all-optical patterning (Figure 2.12). These gratings were found to be significantly large, up to hundreds of nanometers, as confirmed by AFM, which means that the light induced the motion of many hundreds of nanometers of the polymer chains to “walk” across the substrate surface. The SRGs diffract very cleanly and efficiently, and in retrospect, it is clear that many early reports on the large diffraction efficiency prior to 1995, attributed then to birefringence, were in

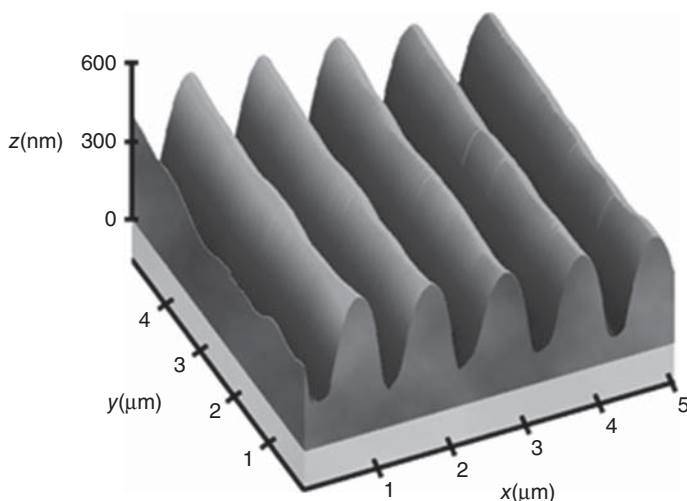


Figure 2.12 AFM image of a typical surface relief grating (SRG) optically inscribed into an azo polymer film. Grating amplitudes of hundreds of nanometers, on the order of the original film thickness, are easily obtained. In this image, the approximate location of the film–substrate interface has been set to $z = 0$, based on the knowledge of the film thickness. (Mahimwalla *et al.* [2]. Reproduced with the permission of Springer.)

fact probably due instead to surface gratings unbeknown to the experimenters. The process occurs readily at room temperature (well below the T_g of the amorphous polymers used) with moderate irradiation ($1\text{--}100\text{ mW/cm}^2$) over seconds to minutes. The phenomenon is a reversible mass transport, not irreversible material ablation, since a flat film with the original thickness is recovered upon heating above T_g . Critically, it requires the presence and isomerization of azobenzene chromophores, as other absorbing but nonisomerizing chromophores do not produce SRGs. Many other systems can exhibit optical surface patterning [167], but the amplitude of the modification is much smaller, does not involve mass transport, and usually requires additional processing steps. The all-optical patterning unique to azobenzenes has been studied intensively since its discovery, and many reviews of the remarkable body of experimental results are available [168–171].

In a typical inscription experiment, a sinusoidally varying light pattern is generated at the sample surface, and what results is a sinusoidal surface profile: an SRG. This is the pattern most often reported in the literature, because it is most conveniently generated (by intersecting two coherent beams) and most easily monitored (by recording the diffraction intensity at a nonabsorbing wavelength, usually using a HeNe laser at 633 nm). However, it must be emphasized that the azo surface mass transport can produce arbitrary patterns. Essentially, the film encodes the impinging light pattern as a topography pattern (as a Fourier transform), holographically encoding both the spatial intensity and the polarization patterns of the incident light. What appears to be essential is a *gradient* in the intensity and/or polarization of the incident light field. For instance, a single focused Gaussian laser spot will lead to a localized pit depression, and a Gaussian line will lead to an elongated trench [172]. In principle, any arbitrary pattern could be generated through an appropriate mask, interference/holographic setup, or laser rastering [170].

Concomitant with the inscription of a surface relief is a photo-orientation of the azo chromophores, which depends on the polarization of the incident beam(s). The orientation of chromophores in SRG experiments has been measured using polarized Raman confocal microspectrometry [173–175], and the strong surface orientation has been confirmed by photoelectron spectroscopy [176]. What is found is that the chromophores orient perpendicular to the local polarization vector of the impinging interference pattern. Thus, for a ($+45^\circ$, -45°) two-beam interference, in the valleys ($x=0$), the electric field is aligned in the y -direction, so the chromophores orient in the x -direction; in the peaks ($x=\Lambda/2$), the chromophores orient in the y -direction; and in the slope regions ($x=\Lambda/4$), the electric field is circularly polarized and thus the chromophores are nearly isotropic. For a (p, p) two-beam interference, it is observed that the chromophores are primarily oriented in the y -direction everywhere, since the impinging light pattern is always linearly polarized in

the x -direction. Mass transport may lead to perturbations in the orientational distribution, but photo-orientation remains the dominant effect.

The anisotropic volume grating that is submerged below a SRG apparently also leads to the formation of a density grating under appropriate conditions. It was found that upon thermal annealing (heating just beyond T_g) of an SRG, which erases the surface grating and restores a flat film surface, a density grating began growing beneath the surface (and into the film bulk) [177, 178]. This density grating only develops where the SRG was originally inscribed, and it appears that the photo-orientation and mass transport lead to the nucleation of liquid-crystalline “seeding aggregates” that are thermally grown into larger scale density variations. The thermal erasure of the SRG, with concomitant growth of the density grating, has been both measured [179] and modeled [180]. The diffraction of a visible-light laser primarily probes the surface relief, whereas a simultaneous X-ray diffraction experiment probes the density grating. The formation of a density grating is similar to, and consistent with, the production of surface topography [181] and surface density patterns [182], as observed by tapping-mode AFM on an azo film exposed to an optical near field. In these experiments, it was found that volume is not strictly conserved during surface deformation [183], consistent with changes in density.

Mass transport effects are not limited to the polymeric azo materials but can also occur in crystals of photochromic molecules. Primarily, such observations represent directional melting and crystal growth as well as self-propulsion in a medium, which is related to the previously discussed photosolient crystals. A first entry into this field was provided by Milam *et al.* with the observation of swimming, sinking, and stationary azobenzene crystals in a triacrylate solution [184]. The motility was rationalized by the creation of concentration/surface tension gradients around the crystal/liquid interface upon exclusion of triacrylate solvent from the growing crystal front. More recently, Hoshino *et al.* demonstrated how irradiation-induced *trans*–*cis* conversion in the crystals of azobenzenes can lead to directed melting of crystals [185]. Simultaneously, Norikane *et al.*, by careful choice of the position and identity of a substituent of on the azobenzene core, have identified the structures amenable to melting by UV light (Figure 2.13) and utilized this phase transition to selectively pattern a copper surface [186]. These observations once again proved the feasibility of reversible *trans*–*cis*-azobenzene isomerization in carefully tailored single crystals.

The observation of light-mediated melting also led to a completely new phenomenon – apparent directional “crawling” of single crystals on a glass surface driven by the melting transition. Upon simultaneous visible and UV irradiation, single crystals of *trans*-3,3'-dimethylazobenzene “crawl” along the flat glass surface (and even vertically) away from the UV light source (Figure 2.14) [187]. The motion is driven by melting and crystallization of the crystals at the front and rear edge, and while the shape of the crystal continuously changes, the

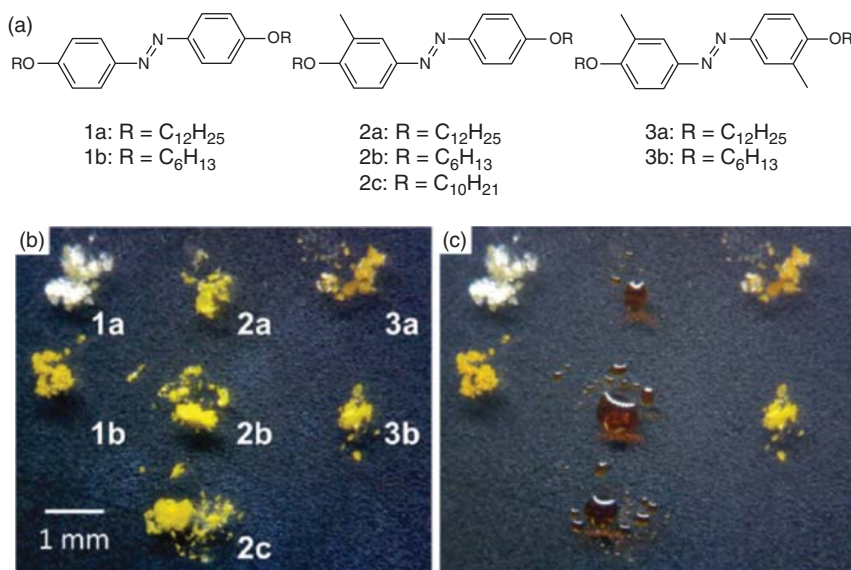


Figure 2.13 (a) Structures and (b) photographs of the crystalline powders of azobenzenes utilized in the study. (c) The same powders after irradiation with 365 nm light for 30 min at 100 mW/cm². (Norikane *et al.* [186]. Reproduced with the permission of American Chemical Society.) (See color plate section for the color representation of this figure.)

optical axis remains constant. Melting-driven motility of crystals is an important step in the development of self-propelled objects [188, 189] and enhances the understanding of crawling phenomenon already observed in photochromic azobenzene-containing glasses and polymers [190, 191]. Such directed surface transport of azobenzene materials is a complimentary (and inverted) observation of the liquid mass transport on the surface of azobenzene-functionalized surfaces pioneered by Ichimura *et al.* [192–194]

2.6 Photochromic Reactions in Framework Architectures

A new avenue of research in solid-state photochromic reactions was opened with the development of metal–organic frameworks (MOFs) and similar network-type crystalline systems [195]. Specifically, upon realization that MOFs can survive in relatively harsh environments and are capable of post-functionalization while retaining very large surface area [196, 197], efforts were made to prepare and study photoswitchable MOFs with the goal of carbon dioxide absorption (Figure 2.15) [198, 199]. Following the idea that azobenzene molecules can only isomerize when used as pendant groups on

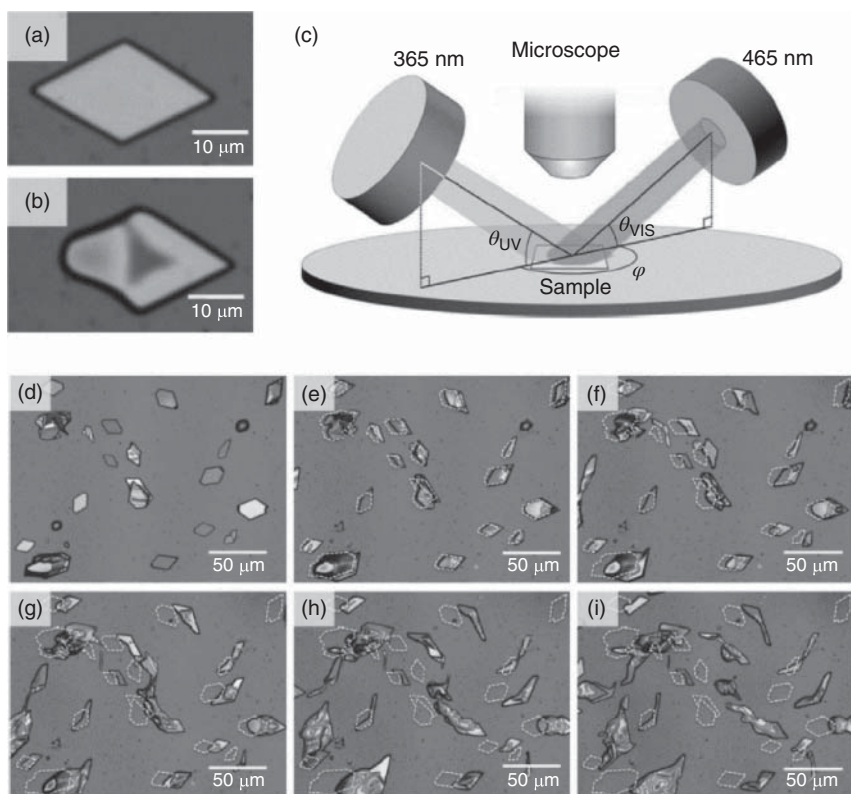


Figure 2.14 (a and b) Motion of single crystals of *trans*-3,3'-dimethylazobenzene on a glass surface. (c) Schematic representation of the irradiation setup; (d–i) microscope images of translational motion of *trans*-3,3'-dimethylazobenzene after irradiation time, t , min 0 (d), 3 (b), 6 (f), 10 (g), 15 (h), 20 (b). Dashed white and dark gray lines represent the initial positions of crystals and droplets, respectively. (Uchida *et al.* [187]. Reproduced with the permission of Nature Publishing Group.)

linkers, photoactive MOFs were prepared and successfully tested to regulate methane absorption [200]. The azobenzene chromophore usually does not act as a truly bistable switch as the lifetime of the *cis* form is usually short. Recently, however, the Hecht group has reported *o*-fluorinated azobenzenes that have lifetimes of a *cis* form of over 2 years in solution [201]. Castellanos *et al.* utilized such fluorinated azobenzenes to prepare a MOF, which is addressable by green and blue light and has potential as a bistable gas-storing material [202].

A simple and elegant approach to photoswitchable gas absorption in MOFs was proposed by Lyndon *et al.* Instead of covalent modification of an MOF or a linker unit, they opted for postsynthetic treatment of the surface of a MOF

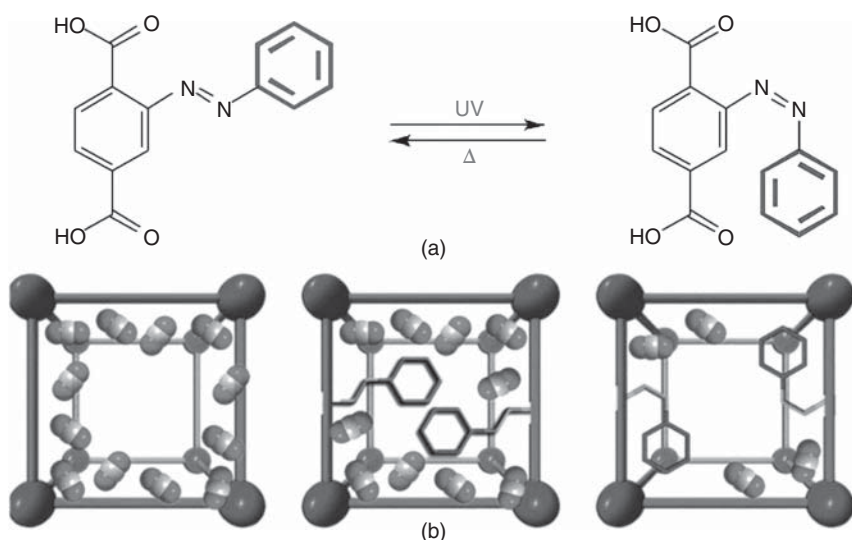


Figure 2.15 (a) Isomerization of the azobenzene ligand within an MOF referred to as PCN-123. (b) Schematic illustration of CO_2 uptake in the parent MOF-5 structure and PCN-123 network in trans and cis states. (Park *et al.* [198]. Reproduced with the permission of American Chemical Society.)

by the azobenzene dye, methyl red. The dye coated the surface and prevented absorption of CO_2 inside the MOF [203]. However, upon irradiation, the pores would open and the MOF absorbed CO_2 . In the same vein, photochromism of azobenzene molecules inside the pores of an MOF was shown by the Kitagawa group to direct structural changes in the network and, as a consequence, regulate gas sorption [204]. Incorporation of azobenzene chromophore as a guest molecule into the network led to a phase change of the network from tetragonal to orthorhombic crystal system upon UV irradiation, which resulted in drastically different uptake profiles. While most of the research is performed under the assumption that switching of azobenzene is only possible in an MOF when chromophores are used as pendant groups [199], a recent report by Baroncini *et al.* may warrant a closer inspection of this idea. Tetrameric star-shaped azobenzene molecules assemble a porous network and then undergo reversible isomerization aided by partial amorphization of the sample [205]. The isomerization in its turn changes the porosity and consequently the gas uptake of the network.

While most of the effort in photoresponsive MOFs was directed toward the study of azobenzene-type chromophores, Walton *et al.* produced photochromic architectures employing diarylethene chromophore [206, 207]. Irradiation of a crystal they refer to as UBMOF-1 with UV light would turn the

crystal red, indicating a successful ring-closure reaction of the diarylethene chromophore. However, unlike in the work by Irie and coworkers on photochromic crystals [109], when diarylethene photochromes are introduced into the MOF scaffold, the reverse reaction can only take place upon digestion of the MOF into its constituents by a strong acid. The reversible switching of diarylethene unit inside a network was since achieved by Luo *et al.*, which allowed light-triggered desorption of up to 75% of CO₂ upon sequential UV and visible irradiation [208].

2.7 Summary and Outlook

As discussed in this chapter, reversible photoisomerization of photochromic molecules in the solid state can be leveraged to control larger scale material properties in response to light. While azobenzene is the most studied of the chromophores, various other photoswitches are increasingly being utilized. Light is an efficient power source for many of these applications, offering a direct conversion of photonic energy into mechanical motion without requirements for energy converters, amplification, or other subsystems. Light is also an ideal triggering mechanism, since it can be localized (in time and space), is selective, nondamaging, and allows remote activation and remote delivery of energy to a system. Thus, for sensing, actuation, and motion, photoresponsive materials are of great interest. Photochromic materials have demonstrated a wide variety of switching behaviors, from altering optical properties, to surface energy changes, to even eliciting bulk material phase changes. Azobenzene is a leader among the small class of photoreversible molecules, and azo crystals, polymers, and other supramolecular azo materials are promising candidates for enabling the potential applications of these systems discussed in this book because of their ease of incorporation and efficient and robust photochemistry. At the same time, for nonpolymeric materials, diarylethenes have shown great promise despite their overall lower fatigue resistance. This chapter described the light-induced effects observed in thin films, crystals, amorphous polymers, and LCNs and LCEs containing various photochromes. The effects range from full macroscopic light-driven actuation to matter transport across the surfaces, phase changes, and modification of gas sorption and storage capacity. The unifying limitation, however, is that the mechanical forces produced thus far and the efficiency for light energy conversion are still far from optimal. LCEs in particular are promising materials for artificial muscles and motors driven by light, and in these systems, not only two-dimensional but also three-dimensional motions have now been achieved, which are competitive and promising for many applications as soft actuators. However, many problems still remain unsolved, such as fatigue resistance and biocompatibility of these materials, which need further intensive investigation.

References

- 1 Yamada, M., Kondo, M., Mamiya, J.I. *et al.* (2008) *Angewandte Chemie, International Edition*, **47**, 4986–4988.
- 2 Mahimwalla, Z., Yager, K.G., Mamiya, J. *et al.* (2012) *Polymer Bulletin*, **69**, 967–1006.
- 3 Bandara, H.M.D. and Burdette, S.C. (2012) *Chemical Society Reviews*, **41**, 1809–1825.
- 4 Wirth, J., Hatter, N., Drost, R. *et al.* (2015) *Journal of Physical Chemistry C*, **119**, 4874–4883.
- 5 Irie, M., Fukaminato, T., Matsuda, K., and Kobatake, S. (2014) *Chemical Reviews*, **114**, 12174–12277.
- 6 Berkovic, G., Krongauz, V., and Weiss, V. (2000) *Chemical Reviews*, **100**, 1741–1753.
- 7 Trenor, S.R., Shultz, A.R., Love, B.J., and Long, T.E. (2004) *Chemical Reviews*, **104**, 3059–3077.
- 8 Whalley, A.C., Steigerwald, M.L., Guo, X., and Nuckolls, C. (2007) *Journal of the American Chemical Society*, **129**, 12590–12591.
- 9 Bauer, J., Hou, L.L., Kistemaker, J.C.M., and Feringa, B.L. (2014) *Journal of Organic Chemistry*, **79**, 4446–4455.
- 10 Su, X., Voskian, S., Hughes, R.P., and Aprahamian, I. (2013) *Angewandte Chemie International Edition*, **52**, 10734–10739.
- 11 Greb, L. and Lehn, J.M. (2014) *Journal of the American Chemical Society*, **136**, 13114–13117.
- 12 Tatum, L.A., Su, X., and Aprahamian, I. (2014) *Accounts of Chemical Research*, **47**, 2141–2149.
- 13 Qu, D.-H., Wang, Q.-C., Zhang, Q.-W. *et al.* (2015) *Chemical Reviews*, **115** (15), 7543–7588.
- 14 Astumian, R.D. (2012) *Nature Nanotechnology*, **7**, 684–688.
- 15 Ichimura, K. (2000) *Chemical Reviews*, **100**, 1847–1873.
- 16 Naito, T., Horie, K., and Mita, I. (1991) *Macromolecules*, **24**, 2907–2911.
- 17 Uznanski, P., Kryszewski, M., and Thulstrup, E.W. (1991) *European Polymer Journal*, **27**, 41–43.
- 18 de Lange, J.J., Robertson, J.M., and Woodward, I. (1939) *Proceedings of the Royal Society of London A*, **A171**, 398–410.
- 19 Hampson, G.C. and Robertson, J.M. (1941) *Journal of the Chemical Society*, 409–413.
- 20 Brown, C.J. (1966) *Acta Cryst*, **21**, 146–152.
- 21 Hartley, G.S. (1937) *Nature*, **140**, 281.
- 22 Naito, T., Horie, K., and Mita, I. (1993) *Polymer*, **34**, 4140–4145.
- 23 Paik, C.S. and Morawetz, H. (1972) *Macromolecules*, **5**, 171–177.
- 24 Lamarre, L. and Sung, C.S.P. (1983) *Macromolecules*, **16**, 1729–1736.

- 25 Weiss, R.G., Ramamurthy, V., and Hammond, G.S. (1993) *Accounts of Chemical Research*, **25**, 530–536.
- 26 Hugel, T., Holland, N.B., Cattani, A. *et al.* (2002) *Science*, **296**, 1103–1106.
- 27 Holland, N.B., Hugel, T., Neuert, G. *et al.* (2003) *Macromolecules*, **36**, 2015–2023.
- 28 Neuert, G., Hugel, T., Netz, R.R., and Gaub, H.E. (2005) *Macromolecules*, **39**, 789–797.
- 29 Tsuchiya, S. (1999) *Journal of American Chemical Society*, **121**, 48–53.
- 30 Steinem, C., Janshoff, A., Vollmer, M.S., and Ghadiri, M.R. (1999) *Langmuir*, **15**, 3956–3964.
- 31 Vollmer, M.S., Clark, T.D., Steinem, C., and Ghadiri, M.R. (1999) *Angewandte Chemie, International Edition*, **38**, 1598–1601.
- 32 Masiero, S., Lena, S., Pieraccini, S., and Spada, G.P. (2008) *Angewandte Chemie, International Edition*, **47**, 3184–3187.
- 33 Fujiwara, M., Akiyama, M., Hata, M. *et al.* (2008) *ACS Nano*, **2**, 1671–1681.
- 34 Pakula, C., Zaporotchenko, V., Strunskus, T. *et al.* (2010) *Nanotechnology*, **21** (46), 465201.
- 35 Raimondo, C., Reinders, F., Soydaner, U. *et al.* (2010) *Chemical Communications*, **46**, 1147–1149.
- 36 Kimoto, A., Iwasaki, K., and Abe, J. (2010) *Photochemical and Photobiological Sciences*, **9**, 152–156.
- 37 Higuchi, M., Minoura, N., and Kinoshita, T. (1995) *Colloid and Polymer Science*, **273**, 1022–1027.
- 38 Siewierski, L.M., Brittain, W.J., Petrash, S., and Foster, M.D. (1996) *Langmuir*, **12**, 5838–5844.
- 39 Stiller, B., Knochenhauer, G., Markava, E. *et al.* (1999) *Materials Science and Engineering: C*, **8–9**, 385–389.
- 40 Moller, G., Harke, M., Motschmann, H., and Prescher, D. (1998) *Langmuir*, **14**, 4955–4957.
- 41 Feng, C.L., Zhang, Y.J., Jin, J. *et al.* (2001) *Langmuir*, **17**, 4593–4597.
- 42 Chen, T., Xu, S., Zhang, F. *et al.* (2009) *Chemical Engineering Science*, **64**, 4350–4357.
- 43 Delorme, N., Bardeau, J.-F., Bulou, A., and Poncin-Epaillard, F. (2005) *Langmuir*, **21**, 12278–12282.
- 44 Diguët, A., Guillermic, R.-M., Magome, N. *et al.* (2009) *Angewandte Chemie, International Edition*, **48**, 9281–9284.
- 45 Sarkar, N., Sarkar, A., and Sivaram, S. (2001) *Journal of Applied Polymer Science*, **81**, 2923–2928.
- 46 Jiang, W.H., Wang, G.J., He, Y.N. *et al.* (2005) *Chemical Communications*, 3550–3552.
- 47 Yu, Y., Nakano, M., and Ikeda, T. (2003) *Nature*, **425**, 145.

- 48 Ikeda, T., Nakano, M., Yu, Y. *et al.* (2003) *Advanced Materials*, **15**, 201–205.
- 49 Yu, Y.L., Nakano, M., Maeda, T. *et al.* (2005) *Molecular Crystals and Liquid Crystals*, **436**, 1235–1244.
- 50 Ji, H.F., Feng, Y., Xu, X.H. *et al.* (2004) *Chemical Communications*, 2532–2533.
- 51 White, T.J., Tabiryan, N.V., Serak, S.V. *et al.* (2008) *Soft Matter*, **4**, 1796–1798.
- 52 White, T.J., Serak, S.V., Tabiryan, N.V. *et al.* (2009) *Journal of Materials Chemistry*, **19**, 1080–1085.
- 53 Serak, S., Tabiryan, N., Vergara, R. *et al.* (2010) *Soft Matter*, **6**, 779–783.
- 54 Deng, W., Li, M.H., Wang, X.G., and Keller, P. (2009) *Liquid Crystals*, **36**, 1023–1029.
- 55 Hrozhyk, U., Serak, S., Tabiryan, N. *et al.* (2009) *Optics Express*, **17**, 716–722.
- 56 Kondo, M., Matsuda, T., Fukae, R., and Kawatsuki, N. (2010) *Chemistry Letters*, **39**, 234–235.
- 57 Cheng, F.T., Zhang, Y.Y., Yin, R.Y., and Yu, Y.L. (2010) *Journal of Materials Chemistry*, **20**, 4888–4896.
- 58 Bai, S. and Zhao, Y. (2001) *Macromolecules*, **34**, 9032–9038.
- 59 Camacho-Lopez, M., Finkelmann, H., Palfy-Muhoray, P., and Shelley, M. (2004) *Nature Materials*, **3**, 307–310.
- 60 Bublitz, D., Helgert, M., Fleck, B. *et al.* (2000) *Applied Physics B*, **70**, 863–865.
- 61 Chen, X., Tao, J., Zou, G. *et al.* (2010) *Applied Physics A: Materials Science & Processing*, **100**, 223–230.
- 62 Merian, E. (1966) *Textile Research Journal*, **36**, 612–618.
- 63 Eisenbach, C.D. (1980) *Polymer*, **21**, 1175–1179.
- 64 Matejka, L., Dusek, K., and Ilavsky, M. (1979) *Polymer Bulletin*, **1**, 659–664.
- 65 Matejka, L. and Dusek, K. (1981) *Makromolekulare Chemie-Macromolecular Chemistry and Physics*, **182**, 3223–3236.
- 66 Matejka, L., Ilavsky, M., Dusek, K., and Wichterle, O. (1981) *Polymer*, **22**, 1511–1515.
- 67 Kim, H.K., Wang, X.S., Fujita, Y. *et al.* (2005) *Macromolecular Rapid Communications*, **26**, 1032–1036.
- 68 Kim, H.K., Wang, X.S., Fujita, Y. *et al.* (2005) *Polymer*, **46**, 5879–5883.
- 69 Kim, H.K., Wang, X.S., Fujita, Y. *et al.* (2005) *Macromolecular Chemistry and Physics*, **206**, 2106–2111.
- 70 Tanaka, S., Kim, H.K., Sudo, A. *et al.* (2008) *Macromolecular Chemistry and Physics*, **209**, 2071–2077.
- 71 Zhang, C., Zhao, X., Chao, D. *et al.* (2009) *Journal of Applied Polymer Science*, **113**, 1330–1334.

- 72 Küpfer, J., Nishikawa, E., and Finkelmann, H. (1994) *Polymers for Advanced Technologies*, **5**, 110–115.
- 73 Wermter, H. and Finkelmann, H. (2001) *e-Polymers*, **1**, 111–123.
- 74 Gennes, P.G.D., Hebert, M., and Kant, R. (1997) *Macromolecular Symposia*, **113**, 39–49.
- 75 Ikeda, T., Mamiya, J., and Yu, Y.L. (2007) *Angewandte Chemie, International Edition*, **46**, 506–528.
- 76 Elias, A.L., Harris, K.D., Bastiaansen, C.W.M. *et al.* (2006) *Journal of Materials Chemistry*, **16**, 2903–2912.
- 77 Yang, H., Ye, G., Wang, X., and Keller, P. (2011) *Soft Matter*, **7**, 815–823.
- 78 Yu, Y., Nakano, M., and Ikeda, T. (2004) *Pure and Applied Chemistry*, **76**, 1467–1477.
- 79 Nakano, H. (2010) *Journal of Materials Chemistry*, **20**, 2071–2074.
- 80 Yoshino, T., Kondo, M., Mamiya, J. *et al.* (2010) *Advanced Materials*, **22**, 1361–1363.
- 81 Kondo, M., Yu, Y., and Ikeda, T. (2006) *Angewandte Chemie, International Edition*, **45**, 1378–1382.
- 82 Tabiryan, N., Serak, S., Dai, X.M., and Bunning, T. (2005) *Optics Express*, **13**, 7442–7448.
- 83 Van Oosten, C.L., Corbett, D., Davies, D. *et al.* (2008) *Macromolecules*, **41**, 8592–8596.
- 84 Priimagi, A., Shimamura, A., Kondo, M. *et al.* (2011) *ACS Macro Letters*, **1**, 96–99.
- 85 Yamada, M., Kondo, M., Miyasato, R. *et al.* (2009) *Journal of Materials Chemistry*, **19**, 60–62.
- 86 Naka, Y., Mamiya, J.-I., Shishido, A. *et al.* (2011) *Journal of Materials Chemistry*, **21**, 1681–1683.
- 87 Yin, R.Y., Xu, W.X., Kondo, M. *et al.* (2009) *Journal of Materials Chemistry*, **19**, 3141–3143.
- 88 Cheng, F., Yin, R., Zhang, Y. *et al.* (2010) *Soft Matter*, **6**, 3447–3449.
- 89 Lee, K.M., Koerner, H., Vaia, R.A. *et al.* (2011) *Soft Matter*, **7**, 4318–4324.
- 90 Wu, W., Yao, L., Yang, T. *et al.* (2011) *Journal of American Chemical Society*, **133**, 15810–15813.
- 91 Harris, K.D., Cuyppers, R., Scheibe, P. *et al.* (2005) *Journal of Materials Chemistry*, **15**, 5043–5048.
- 92 Kondo, M., Sugimoto, M., Yamada, M. *et al.* (2010) *Journal of Materials Chemistry*, **20**, 117–122.
- 93 Lee, K.M., Koerner, H., Vaia, R.A. *et al.* (2010) *Macromolecules*, **43**, 8185–8190.
- 94 Shimamura, A., Priimagi, A., Mamiya, J.-I. *et al.* (2011) *Journal of Nonlinear Optical Physics and Materials*, **20**, 405–413.
- 95 Liu, D. and Broer, D.J. (2015) *Nature Communications*, **6**, Article number: 8334.

- 96 Ionov, L. (2015) *Langmuir*, **31**, 5015–5024.
- 97 Ware, T.H., McConney, M.E., Wie, J.J. *et al.* (2015) *Science*, **347**, 982–984.
- 98 Iamsaard, S., Aßhoff, S.J., Matt, B. *et al.* (2014) *Nature Chemistry*, **6**, 229–235.
- 99 Dunitz, J.D., Schomaker, V., and Trueblood, K.N. (1988) *Journal of Physical Chemistry*, **92**, 856–867.
- 100 Nath, N.K., Panda, M.K., Sahoo, S.C., and Naumov, P. (2014) *CrystEngComm*, **16**, 1850–1858.
- 101 Lange, C.W., Foldeaki, M., Nevodchikov, V.I. *et al.* (1992) *Journal of the American Chemical Society*, **114**, 4220–4222.
- 102 Naumov, P., Sahoo, S.C., Zakharov, B.A., and Boldyreva, E.V. (2013) *Angewandte Chemie International Edition*, **52**, 9990–9995.
- 103 Kim, T., Zhu, L., Al-Kaysi, R.O., and Bardeen, C.J. (2014) *ChemPhysChem*, **15**, 400–414.
- 104 Panda, M.K., Runcevski, T., Sahoo, S.C. *et al.* (2014) *Nature Communications*, **5**, 4811.
- 105 Sahoo, S.C., Panda, M.K., Nath, N.K., and Naumov, P. (2013) *Journal of American Chemical Society*, **135**, 12241–12251.
- 106 Sahoo, S.C., Sinha, S.B., Kiran, M.S.R.N. *et al.* (2013) *Journal of American Chemical Society*, **135**, 13843–13850.
- 107 Medishetty, R., Husain, A., Bai, Z.Z. *et al.* (2014) *Angewandte Chemie International Edition*, **53**, 5907–5911.
- 108 Sahoo, S.C., Nath, N.K., Zhang, L.D. *et al.* (2014) *RSC Advances*, **4**, 7640–7647.
- 109 Kobatake, S., Takami, S., Muto, H. *et al.* (2007) *Nature*, **446**, 778–781.
- 110 Kitagawa, D. and Kobatake, S. (2014) *Photochemical & Photobiological Sciences*, **13**, 764–769.
- 111 Morimoto, M. and Irie, M. (2010) *Journal of American Chemical Society*, **132**, 14172–14178.
- 112 Terao, F., Morimoto, M., and Irie, M. (2012) *Angewandte Chemie International Edition*, **51**, 901–904.
- 113 Kitagawa, D. and Kobatake, S. (2015) *Chemical Communications*, **51**, 4421–4424.
- 114 Zhu, L.Y., Al-Kaysi, R.O., and Bardeen, C.J. (2011) *Journal of American Chemical Society*, **133**, 12569–12575.
- 115 Kim, T., Al-Muhanna, M.K., Al-Suwaidan, S.D. *et al.* (2013) *Angewandte Chemie International Edition*, **52**, 6889–6893.
- 116 Kim, T., Zhu, L.C., Mueller, L.J., and Bardeen, C.J. (2014) *Journal of American Chemical Society*, **136**, 6617–6625.
- 117 Koshima, H., Matsuo, R., Matsudomi, M. *et al.* (2013) *Crystal Growth & Design*, **13**, 4330–4337.
- 118 Kumar, A.S., Ye, T., Takami, T. *et al.* (2008) *Nano Letters*, **8**, 1644–1648.

- 119 Zheng, Y.B., Payton, J.L., Chung, C.H. *et al.* (2011) *Nano Letters*, **11**, 3447–3452.
- 120 Vapaavuori, J., Goulet-Hanssens, A., Heikkinen, I.T.S. *et al.* (2014) *Chemistry of Materials*, **26**, 5089–5096.
- 121 Goulet-Hanssens, A. and Barrett, C.J. (2013) *Journal of Polymer Science Part A: Polymer Chemistry*, **51**, 3058–3070.
- 122 Ikeda, T. and Tsutsumi, O. (1995) *Science*, **268**, 1873–1875.
- 123 Koshima, H., Ojima, N., and Uchimoto, H. (2009) *Journal of American Chemical Society*, **131**, 6890–6891.
- 124 Bushuyev, O.S., Singleton, T.A., and Barrett, C.J. (2013) *Advanced Materials*, **25**, 1796–1800.
- 125 Bushuyev, O.S., Tomberg, A., Friscic, T., and Barrett, C.J. (2013) *Journal of American Chemical Society*, **135**, 12556–12559.
- 126 Bushuyev, O.S., Corkery, T.C., Barrett, C.J., and Friscic, T. (2014) *Chemical Science*, **5**, 3158–3164.
- 127 Warner, M. and Mahadevan, L. (2004) *Physical Review Letters*, **92**, 134302.
- 128 Nath, N.K., Pejov, L., Nichols, S.M. *et al.* (2014) *Journal of American Chemical Society*, **136**, 2757–2766.
- 129 Mahadevan, L. and Matsudaira, P. (2000) *Science*, **288**, 95–99.
- 130 Asimov, I. (1942) *Astounding Science-Fiction*, **1**, 94.
- 131 Kay, E.R., Leigh, D.A., and Zerbetto, F. (2007) *Angewandte Chemie International Edition*, **46**, 72–191.
- 132 Coskun, A., Banaszak, M., Astumian, R.D. *et al.* (2012) *Chemical Society Reviews*, **41**, 19–30.
- 133 Abendroth, J.M., Bushuyev, O.S., Weiss, P.S., and Barrett, C.J. (2015) *ACS Nano*, **9**, 7746–7768.
- 134 Baudrion, A.L., Perron, A., Veltri, A. *et al.* (2013) *Nano Letters*, **13**, 282–286.
- 135 Zheng, Y.B., Kiraly, B., Cheunkar, S. *et al.* (2011) *Nano Letters*, **11**, 2061–2065.
- 136 Joshi, G.K., Blodgett, K.N., Muhoberac, B.B. *et al.* (2014) *Nano Letters*, **14**, 532–540.
- 137 Lee, J.-W. and Klajn, R. (2015) *Chemical Communications*, **51**, 2036–2039.
- 138 Klajn, R., Stoddart, J.F., and Grzybowski, B.A. (2010) *Chemical Society Reviews*, **39**, 2203–2237.
- 139 Swaminathan, S., Garcia-Amorós, J., Fraix, A. *et al.* (2014) *Chemical Society Reviews*, **43**, 4167–4178.
- 140 Song, N. and Yang, Y.-W. (2015) *Chemical Society Reviews*, **44**, 3474–3504.
- 141 Mal, N.K., Fujiwara, M., and Tanaka, Y. (2003) *Nature*, **421**, 350–353.
- 142 Guardado-Alvarez, T.M., Devi, L.S., Russell, M.M. *et al.* (2013) *Journal of the American Chemical Society*, **135**, 14000–14003.
- 143 Mei, X., Yang, S., Chen, D.Y. *et al.* (2012) *Chemical Communications*, **48**, 10010–10012.

- 144 Li, T., Lohmann, F., and Famulok, M. (2014) *Nature Communications*, **5**, Article number: 4279.
- 145 Yang, Y.W. (2011) *MedChemComm*, **2**, 1033–1049.
- 146 Croissant, J., Maynadier, M., Gallud, A. *et al.* (2013) *Angewandte Chemie International Edition*, **52**, 13813–13817.
- 147 Croissant, J., Chaix, A., Mongin, O. *et al.* (2014) *Small*, **10**, 1752–1755.
- 148 Gary-Bobo, M., Mir, Y., Rouxel, C. *et al.* (2011) *Angewandte Chemie International Edition*, **50**, 11425–11429.
- 149 Bléger, D., Dokić, J., Peters, M.V. *et al.* (2011) *The Journal of Physical Chemistry B*, **115**, 9930–9940.
- 150 Bleger, D., Liebig, T., Thiermann, R. *et al.* (2011) *Angewandte Chemie International Edition*, **50**, 12559–12563.
- 151 Lee, C.L., Liebig, T., Hecht, S. *et al.* (2014) *ACS Nano*, **8**, 11987–11993.
- 152 Wie, J.J., Chatterjee, S., Wang, D.H. *et al.* (2014) *Polymer*, **55**, 5915–5923.
- 153 Fang, L.J., Zhang, H.T., Li, Z.D. *et al.* (2013) *Macromolecules*, **46**, 7650–7660.
- 154 Crivillers, N., Osella, S., Van Dyck, C. *et al.* (2013) *Advanced Materials*, **25**, 432–436.
- 155 Zheng, Y.B., Yang, Y.W., Jensen, L. *et al.* (2009) *Nano Letters*, **9**, 819–825.
- 156 Chen, M. and Besenbacher, F. (2011) *ACS Nano*, **5**, 1549–1555.
- 157 Ahmad, N.M., Lu, X.Y., and Barrett, C.J. (2010) *Journal of Materials Chemistry*, **20**, 244–247.
- 158 Patra, D., Zhang, H., Sengupta, S., and Sen, A. (2013) *ACS Nano*, **7**, 7674–7679.
- 159 Zasadzinski, J.A., Viswanathan, R., Madsen, L. *et al.* (1994) *Science*, **263**, 1726–1733.
- 160 Pathem, B.K., Claridge, S.A., Zheng, Y.B., and Weiss, P.S. (2013) *Annual Review of Physical Chemistry*, **64**, 605–630.
- 161 Tegeder, P. (2012) *Journal of Physics: Condensed Matter*, **24**, 394001.
- 162 Pathem, B.K., Zheng, Y.B., Payton, J.L. *et al.* (2012) *Journal of Physical Chemistry Letters*, **3**, 2388–2394.
- 163 Chen, K.Y., Ivashenko, O., Carroll, G.T. *et al.* (2014) *Journal of American Chemical Society*, **136**, 3219–3224.
- 164 London, G., Chen, K.Y., Carroll, G.T., and Feringa, B.L. (2013) *Chemistry--A European Journal*, **19**, 10690–10697.
- 165 Rochon, P., Batalla, E., and Natansohn, A. (1995) *Applied Physics Letters*, **66**, 136–138.
- 166 Kim, D.Y., Tripathy, S.K., Li, L., and Kumar, J. (1995) *Applied Physics Letters*, **66**, 1166–1168.
- 167 Yamaki, S., Nakagawa, M., Morino, S., and Ichimura, K. (2000) *Applied Physics Letters*, **76**, 2520–2522.
- 168 Delaire, J.A. and Nakatani, K. (2000) *Chemical Reviews*, **100**, 1817–1846.

- 169 Viswanathan, N.K., Kim, D.Y., Bian, S. *et al.* (1999) *Journal of Materials Chemistry*, **9**, 1941–1955.
- 170 Natansohn, A. and Rochon, P. (2002) *Chemical Reviews*, **102**, 4139–4176.
- 171 Yager, K.G. and Barrett, C.J. (2001) *Current Opinion in Solid State & Materials Science*, **5**, 487–494.
- 172 Bian, S., Li, L., Kumar, J. *et al.* (1998) *Applied Physics Letters*, **73**, 1817–1819.
- 173 Labarthe, F.L., Bruneel, J.L., Buffeteau, T., and Sourisseau, C. (2004) *Journal of Physical Chemistry B*, **108**, 6949–6960.
- 174 Lagugne-Labarthe, F., Bruneel, J.L., Rodriguez, V., and Sourisseau, C. (2004) *Journal of Physical Chemistry B*, **108**, 1267–1278.
- 175 Labarthe, F.L., Bruneel, J.L., Buffeteau, T. *et al.* (2000) *Physical Chemistry Chemical Physics*, **2**, 5154–5167.
- 176 Henneberg, O., Geue, T., Pietsch, U. *et al.* (2004) *Applied Physics Letters*, **84**, 1561–1563.
- 177 Pietsch, U., Rochon, P., and Natansohn, A. (2000) *Advanced Materials*, **12**, 1129–1132.
- 178 Geue, T., Henneberg, O., Grenzer, J. *et al.* (2002) *Colloids and Surfaces A*, **198-200**, 31–36.
- 179 Geue, T.M., Saphiannikova, M.G., Henneberg, O. *et al.* (2003) *Journal of Applied Physics*, **93**, 3161–3166.
- 180 Pietsch, U. (2002) *Physical Review B*, **66**, 155430.
- 181 Watanabe, O., Ikawa, T., Hasegawa, M. *et al.* (2000) *Molecular Crystals and Liquid Crystals*, **345**, 629–634.
- 182 Ikawa, T., Mitsuoka, T., Hasegawa, M. *et al.* (2000) *Journal of Physical Chemistry B*, **104**, 9055–9058.
- 183 Keum, C.D., Ikawa, T., Tsuchimori, M., and Watanabe, O. (2003) *Macromolecules*, **36**, 4916–4923.
- 184 Milam, K., O'Malley, G., Kim, N. *et al.* (2010) *Journal of Physical Chemistry B*, **114**, 7791–7796.
- 185 Hoshino, M., Uchida, E., Norikane, Y. *et al.* (2014) *Journal of the American Chemical Society*, **136**, 9158–9164.
- 186 Norikane, Y., Uchida, E., Tanaka, S. *et al.* (2014) *Organic Letters*, **16**, 5012–5015.
- 187 Uchida, E., Azumi, R., and Norikane, Y. (2015) *Nature Communications*, **6**, Article number: 7310.
- 188 Nakata, S., Hata, M., Ikura, Y.S. *et al.* (2013) *Journal of Physical Chemistry C*, **117**, 24490–24495.
- 189 Nagai, K.H., Sumino, Y., Montagne, R. *et al.* (2015) *Physical Review Letters*, **114**, 168001.
- 190 Suzuki, M. and Nakano, H. (2012) *Journal of Photopolymer Science and Technology*, **25**, 159–160.

- 191 Nakano, H. and Suzuki, M. (2012) *Journal of Materials Chemistry*, **22**, 3702–3704.
- 192 Ichimura, K., Oh, S.K., and Nakagawa, M. (2000) *Science*, **288**, 1624–1626.
- 193 Oh, S.-K., Nakagawa, M., and Ichimura, K. (2002) *Journal of Materials Chemistry*, **12**, 2262–2269.
- 194 Kausar, A., Nagano, H., Ogata, T. *et al.* (2009) *Angewandte Chemie, International Edition*, **48**, 2144–2147.
- 195 Yaghi, O.M. and Li, H. (1995) *Journal of American Chemical Society*, **117**, 10401–10402.
- 196 Li, H., Eddaoudi, M., O’Keeffe, M., and Yaghi, O.M. (1999) *Nature*, **402**, 276–279.
- 197 Chui, S.S.-Y., Lo, S.M.-F., Charmant, J.P.H. *et al.* (1999) *Science*, **283**, 1148–1150.
- 198 Park, J., Yuan, D., Pham, K.T. *et al.* (2012) *Journal of American Chemical Society*, **134**, 99–102.
- 199 Modrow, A., Zargarani, D., Herges, R., and Stock, N. (2011) *Dalton Transactions*, **40**, 4217–4222.
- 200 Modrow, A., Zargarani, D., Herges, R., and Stock, N. (2012) *Dalton Transactions*, **41**, 8690–8696.
- 201 Bléger, D., Schwarz, J., Brouwer, A.M., and Hecht, S. (2012) *Journal of the American Chemical Society*, **134**, 20597–20600.
- 202 Castellanos, S., Goulet-Hanssens, A., Zhao, F. *et al.* (2016) *Chemistry – A European Journal*, **22**, 746–752.
- 203 Lyndon, R., Konstas, K., Thornton, A.W. *et al.* (2015) *Chemistry of Materials*, **27**, 7882–7888.
- 204 Yanai, N., Uemura, T., Inoue, M. *et al.* (2012) *Journal of American Chemical Society*, **134**, 4501–4504.
- 205 Baroncini, M., d’Agostino, S., Bergamini, G. *et al.* (2015) *Nature Chemistry*, **7**, 634–640.
- 206 Walton, I.M., Cox, J.M., Coppin, J.A. *et al.* (2013) *Chemical Communications*, **49**, 8012–8014.
- 207 Patel, D.G., Walton, I.M., Cox, J.M. *et al.* (2014) *Chemical Communications*, **50**, 2653–2656.
- 208 Luo, F., Fan, C.B., Luo, M.B. *et al.* (2014) *Angewandte Chemie, International Edition*, **126**, 9452–9455.